The Astrophysical Journal Supplement Series, 227:16 (17pp), 2016 December doi:10.3847/0067-0049/227/2/16

EXTENDED CALCULATIONS WITH SPECTROSCOPIC ACCURACY: ENERGY LEVELS AND TRANSITION PROPERTIES FOR THE FLUORINE-LIKE ISOELECTRONIC SEQUENCE WITH $Z = 24$–30

R. Si[1,2], S. Li[3], X. L. Guo[4], Z. B. Chen[5], T. Brage[2], P. Jönsson[6], K. Wang[7], J. Yan[3,8,9], C. Y. Chen[1], and Y. M. Zou[1]
[1] Shanghai EBIT Lab, Institute of Modern Physics, Department of Nuclear Science and Technology, Fudan University, Shanghai 200433, China; chychen@fudan.edu.cn
[2] Division of Mathematical Physics, Department of Physics, Lund University, Box 118, SE-22100 Lund, Sweden
[3] Institute of Applied Physics and Computational Mathematics, Beijing 100088, China
[4] Department of Radiotherapy, Shanghai Changhai Hospital, Second Military Medical University, Shanghai 200433, Peoples Republic Of China
[5] College of Science, National University of Defense Technology, Changsha 410073, China
[6] Group for Materials Science and Applied Mathematics, Malmö University, SE-20506, Malmö, Sweden
[7] Hebei Key Lab of Optic-electronic Information and Materials, The College of Physics Science and Technology, Hebei University, Baoding 071002, China; wang_kai10@fudan.edu.cn
[8] Center for Applied Physics and Technology, Peking University, Beijing 100871, China
[9] Collaborative Innovation Center of IFSA (CICIFSA), Shanghai Jiao Tong University, Shanghai 200240, China
Received 2016 August 26; revised 2016 October 17; accepted 2016 October 25; published 2016 December 2

ABSTRACT

We have performed extensive multiconfiguration Dirac–Hartree–Fock calculations and second-order many-body perturbation calculations for F-like ions with $Z = 24$–30. Energy levels and transition rates for electric dipole (E1), electric-quadrupole (E2), electric-octupole (E3), magnetic dipole (M1), and magnetic-quadrupole (M2) transitions, as well as radiative lifetimes, are provided for the lowest 200 levels belonging to the $1s^22s^22p^5$, $1s^22s2p^6$, $1s^22s^22p^43l$, $1s^22s2p^53l$, $1s^22p^63l$, and $1s^22s^22p^44l$ configurations of each ion. The results from the two sets of calculations are in excellent agreement. Extensive comparisons are also made with other theoretical results and observed data from the CHIANTI and NIST databases. The present energies and wavelengths are believed to be accurate enough to aid line identifications involving the $n = 3$ and $n = 4$ configurations, for which observations are largely missing. The calculated wavelengths and transition data will be useful in the modeling and diagnostics of astrophysical and fusion plasmas.

Key words: atomic data – atomic processes

Supporting material: machine-readable tables

1. INTRODUCTION

Accurately known atomic data, such as energy levels and radiative transition properties, are not only important for basic atomic physics, but also for applications to diagnostics of plasmas. The spectra of F-like ions, especially for medium Z ions, including the iron period elements, are often observed in both astrophysical (e.g., Feldman et al. 1998, 2000; Ko et al. 2002; Curdt et al. 2004; Landi & Phillips 2005; Doschek & Feldman 2010; Shestov et al. 2014) and laboratory plasmas (e.g., Gu et al. 2007a, 2007b; Ouart et al. 2011; Safronova et al. 2012; Beiersdorfer et al. 2014). Using specific spectral lines, one can obtain the most fundamental properties of the plasma, such as ionization state, electron temperature, electron density, and elemental abundances. For example, Fe XVIII emission lines of the $n = 3, 4 \rightarrow 2$ transitions have been suggested to diagnose temperatures for a wide range of "hot" astrophysical sources, while the $n = 2, 3 \rightarrow 2$ transitions can be used to measure electron densities in laboratory plasmas (Cornille et al. 1992; Warren et al. 1997; Del Zanna 2006). The ratios of the Fe XVIII $n = 3 \rightarrow 2$ DR satellites to the parent lines are also of interest for temperature measurements of cool stars (Clementson & Beiersdorfer 2013). The Ni L-shell lines can also become important for deblending the neighboring Fe lines and providing additional measurement constraints (Gu et al. 2007a, 2007b). It is clear that accurate line interpretation and plasma modeling rely heavily on comprehensive and accurate atomic data.

There is a wealth of theoretical studies on atomic data of F-like ions. Most of them are confined to low-lying states and only include a limited treatment of electron correlation effects (e.g., Cheng et al. 1979; Kim & Huang 1982; Edlén 1983; Mohan & Hibbert 1991; Blackford & Hibbert 1994). Gu (2005a) determined level energies of $1s^22s^22p^5$, and $1s^22s2p^6$ configurations for F-like ions with $Z \leqslant 60$ using a combined configuration interaction and many-body perturbation theory. Jönsson et al. (2013a) reported transition energies and transition rates of the $n = 2$ configurations for F-like ions with $Z = 14$–74 using the multiconfiguration Dirac–Hartree–Fock (MCDHF) method as implemented in the GRASP2K code (Jönsson et al. 2007). Employing an all-order perturbative method, Nandy & Sahoo (2014) also provided atomic data of the first two excited states for F-like Ti, V, Cr, Mn, Co, Ni, Cu, Zn, and Mo ions.

It is clear that atomic data for higher-lying levels of $n = 3, 4$ configurations are also important on account of their wide applications in plasma diagnostics (Phillips et al. 1982; Cornille et al. 1992; Warren et al. 1997; Del Zanna 2006; Clementson & Beiersdorfer 2013). Jonauskas et al. (2004) presented excitation energies for the 379 lowest bound levels for Fe XVIII, along with multipole transition probabilities between these levels based on calculations with the multiconfiguration Dirac-Fock GRASP code of Dyall et al. (1989). Using a combined configuration interaction and many-body perturbation theory approach, Gu (2005b) calculated level energies of the $1s^22l^7$ and $1s^22l^63l'$ complexes in F-like Fe and Ni ions, as well as wavelengths of $n \rightarrow 2$ (where $3 \leqslant n \leqslant 7$) transitions for Fe and Ni L-shell ions (Gu 2007). Witthoeft et al. (2006, 2007) presented R-matrix collision strengths for

Table 1
Energy Levels (in cm^{-1}) Relative to the Ground State and Lifetimes (τ in s) for the Lowest 200 Levels of F-like Ions with $Z = 24$–30

Z	Key	Configuration	Term	E_{NIST}	E_{MCDHF}	E_{MBPT}	τ_{MCDHF}	τ_{MBPT}	Composition
26	1	$2s^22p^5$	$^2P_{3/2}$	0	0	0	⋯	⋯	99.9 (1)
26	2	$2s^22p^5$	$^2P_{1/2}$	102579	102624	102700	5.16E−05	5.18E−05	99.9 (2)
26	3	$2s2p^6$	$^2S_{1/2}$	1064702	1064636	1063301	9.45E−12	9.56E−12	99.8 (3)
26	4	$2s^22p^4(^3P)3s$	$^4P_{5/2}$	6222000	6220453	6221703	1.20E−11	1.21E−11	91.3 (4)
26	5	$2s^22p^4(^3P)3s$	$^2P_{3/2}$	6248100	6247489	6248466	6.04E−13	6.06E−13	57.5 (5) 31.1 (7) 11.1 (10)
26	6	$2s^22p^4(^3P)3s$	$^4P_{1/2}$	6310200	6299521	6300787	5.71E−12	5.74E−12	83.5 (6)
26	7	$2s^22p^4(^3P)3s$	$^4P_{3/2}$	6317900	6317185	6318306	1.16E−12	1.18E−12	67.7 (7) 30.4 (5) 1.50 (10)
26	8	$2s^22p^4(^3P)3s$	$^2P_{1/2}$	6342600	6342298	6343151	3.97E−13	4.00E−13	90.1 (8)
26	9	$2s^22p^4(^1D)3s$	$^2D_{5/2}$	6400000	6399342	6400267	1.03E−12	1.03E−12	91.2 (9)
26	10	$2s^22p^4(^1D)3s$	$^2D_{3/2}$	6403800	6403198	6404088	8.25E−13	8.31E−13	87.0 (10)
26	11	$2s^22p^4(^3P)3p$	$^4P_{3/2}$	⋯	6465739	6466794	2.33E−10	2.36E−10	60.0 (11) 12.3 (22) 8.79 (29)
26	12	$2s^22p^4(^3P)3p$	$^4P_{5/2}$	⋯	6469211	6470313	2.75E−10	2.78E−10	66.1 (12) 24.6 (21) 4.50 (28)
26	13	$2s^22p^4(^3P)3p$	$^4P_{1/2}$	⋯	6496588	6497547	1.95E−10	1.98E−10	39.1 (13) 22.0 (23) 20.1 (30)
26	14	$2s^22p^4(^3P)3p$	$^4D_{7/2}$	⋯	6501641	6502697	1.80E−10	1.82E−10	90.0 (14)
26	15	$2s^22p^4(^3P)3p$	$^2D_{5/2}$	⋯	6502489	6503384	1.85E−10	1.86E−10	60.5 (15) 14.6 (12) 13.1 (21)
26	16	$2s^22p^4(^3P)3p$	$^4D_{1/2}$	⋯	6554009	6555046	2.64E−10	2.68E−10	50.2 (16) 23.0 (13) 11.0 (23)
26	17	$2s^22p^4(^3P)3p$	$^4D_{3/2}$	⋯	6555008	6555818	1.46E−10	1.46E−10	41.5 (17) 21.1 (24) 16.0 (22)
26	18	$2s^22p^4(^3P)3p$	$^2S_{1/2}$	⋯	6557024	6558007	1.31E−10	1.33E−10	31.9 (13) 28.7 (18) 24.2 (16)
26	19	$2s^22p^4(^1S)3s$	$^2S_{1/2}$	6575100	6557571	6558683	9.36E−13	9.47E−13	78.0 (19)
26	20	$2s^22p^4(^3P)3p$	$^2P_{3/2}$	⋯	6571948	6572833	1.72E−10	1.75E−10	43.0 (17) 23.7 (20) 10.1 (22)
26	21	$2s^22p^4(^3P)3p$	$^4D_{5/2}$	⋯	6588725	6589750	1.82E−10	1.84E−10	58.2 (21) 25.2 (15) 14.7 (12)
26	22	$2s^22p^4(^3P)3p$	$^4S_{3/2}$	⋯	6591601	6592529	8.34E−11	8.47E−11	29.5 (22) 26.3 (11) 18.8 (29)
26	23	$2s^22p^4(^3P)3p$	$^2P_{1/2}$	⋯	6607736	6608570	1.93E−10	1.96E−10	51.2 (18) 17.3 (23) 15.3 (16)
26	24	$2s^22p^4(^3P)3p$	$^2D_{3/2}$	⋯	6613421	6614245	1.25E−10	1.27E−10	61.2 (24) 25.1 (22) 4.45 (20)
26	25	$2s^22p^4(^1D)3p$	$^2F_{5/2}$	⋯	6646356	6647125	2.22E−10	2.25E−10	80.9 (25)
26	26	$2s^22p^4(^1D)3p$	$^2F_{7/2}$	⋯	6667816	6668602	1.74E−10	1.76E−10	90.0 (26)
26	27	$2s^22p^4(^1D)3p$	$^2D_{3/2}$	⋯	6683061	6683837	9.54E−11	9.63E−11	81.8 (27)
26	28	$2s^22p^4(^1D)3p$	$^2D_{5/2}$	⋯	6695348	6696131	1.38E−10	1.39E−10	84.6 (28)
26	29	$2s^22p^4(^1D)3p$	$^2P_{3/2}$	⋯	6738826	6737502	2.18E−11	2.27E−11	47.7 (29) 39.7 (20) 6.22 (27)
26	30	$2s^22p^4(^1D)3p$	$^2P_{1/2}$	⋯	6762929	6762769	1.40E−11	1.44E−11	50.4 (30) 22.3 (38) 18.7 (23)
26	31	$2s^22p^4(^3P)3d$	$^4D_{5/2}$	⋯	6804385	6805220	1.22E−10	1.25E−10	73.7 (31)
26	32	$2s^22p^4(^3P)3d$	$^4D_{7/2}$	⋯	6804564	6805386	1.40E−10	1.42E−10	76.2 (32)
26	33	$2s^22p^4(^3P)3d$	$^4D_{3/2}$	⋯	6809996	6810824	1.83E−11	1.82E−11	63.1 (33) 16.8 (40) 6.37 (57)
26	34	$2s^22p^4(^3P)3d$	$^4D_{1/2}$	⋯	6819134	6819919	1.84E−11	1.85E−11	48.1 (34) 18.5 (39) 18.5 (42)
26	35	$2s^22p^4(^3P)3d$	$^4F_{9/2}$	⋯	6828304	6828973	1.27E−10	1.29E−10	89.1 (35)
26	36	$2s^22p^4(^1S)3p$	$^2P_{3/2}$	⋯	6836243	6837183	4.25E−11	4.30E−11	79.0 (36)
26	37	$2s^22p^4(^3P)3d$	$^2F_{7/2}$	⋯	6839004	6839400	1.13E−10	1.14E−10	58.7 (37) 26.7 (45) 12.8 (50)
26	38	$2s^22p^4(^1S)3p$	$^2P_{1/2}$	⋯	6850099	6849608	8.07E−11	8.53E−11	54.6 (38) 28.6 (23) 7.37 (30)
26	39	$2s^22p^4(^3P)3d$	$^4P_{1/2}$	6858200	6855622	6856308	3.66E−13	3.67E−13	64.4 (39) 20.6 (42) 9.64 (52)
26	40	$2s^22p^4(^3P)3d$	$^4P_{3/2}$	6872400	6870934	6871560	2.51E−13	2.51E−13	49.2 (40) 27.5 (46) 9.76 (57)
26	41	$2s^22p^4(^3P)3d$	$^2F_{5/2}$	6880400	6878734	6879107	2.15E−13	2.15E−13	27.3 (41) 22.8 (49) 21.4 (47)
26	42	$2s^22p^4(^3P)3d$	$^2P_{1/2}$	6903200	6898206	6898912	3.45E−12	3.51E−12	49.4 (34) 27.9 (42) 14.4 (58)
26	43	$2s^22p^4(^3P)3d$	$^4F_{3/2}$	⋯	6902518	6903232	1.31E−12	1.33E−12	74.4 (43)
26	44	$2s^22p^4(^3P)3d$	$^4F_{5/2}$	6903700	6904049	6904847	1.14E−10	1.17E−10	53.1 (44) 18.7 (47) 12.7 (60)
26	45	$2s^22p^4(^3P)3d$	$^4F_{7/2}$	⋯	6913250	6913878	1.30E−10	1.32E−10	52.3 (45) 26.1 (37) 19.1 (32)
26	46	$2s^22p^4(^3P)3d$	$^2D_{3/2}$	6919000	6917645	6918302	6.38E−13	6.52E−13	27.2 (33) 21.2 (40) 19.1 (46)
26	47	$2s^22p^4(^3P)3d$	$^4P_{5/2}$	⋯	6933490	6934104	2.41E−12	2.55E−12	43.6 (47) 34.9 (41) 9.60 (44)
26	48	$2s^22p^4(^3P)3d$	$^2P_{3/2}$	6947300	6946084	6946622	7.30E−13	7.24E−13	49.8 (48) 20.3 (55) 9.52 (46)
26	49	$2s^22p^4(^3P)3d$	$^2D_{5/2}$	6957500	6956007	6956246	1.42E−13	1.42E−13	44.9 (49) 28.9 (41) 11.3 (56)
26	50	$2s^22p^4(^1D)3d$	$^2G_{7/2}$	⋯	6985848	6986080	1.18E−10	1.20E−10	85.4 (50)
26	51	$2s^22p^4(^1D)3d$	$^2G_{9/2}$	⋯	6988331	6988608	1.37E−10	1.39E−10	89.1 (51)
26	52	$2s^22p^4(^1D)3d$	$^2S_{1/2}$	7014300	7013324	7013557	5.95E−14	6.00E−14	83.9 (52)
26	53	$2s^22p^4(^1D)3d$	$^2F_{5/2}$	⋯	7013527	7013968	7.01E−13	7.01E−13	59.6 (53) 35.4 (56) 2.01 (44)
26	54	$2s^22p^4(^1D)3d$	$^2F_{7/2}$	⋯	7024270	7024667	1.11E−10	1.13E−10	90.1 (54)
26	55	$2s^22p^4(^1D)3d$	$^2P_{3/2}$	7038400	7037342	7037576	4.77E−14	4.84E−14	67.5 (55) 19.1 (48) 4.71 (61)
26	56	$2s^22p^4(^1D)3d$	$^2D_{5/2}$	7040800	7041084	7040954	5.54E−14	5.68E−14	44.0 (56) 26.3 (53) 22.4 (49)
26	57	$2s^22p^4(^1D)3d$	$^2D_{3/2}$	7066100	7065732	7065539	5.88E−14	5.94E−14	67.6 (57) 25.8 (46) 3.24 (61)

Table 1
(Continued)

Z	Key	Configuration	Term	$E_{\rm NIST}$	$E_{\rm MCDHF}$	$E_{\rm MBPT}$	$\tau_{\rm MCDHF}$	$\tau_{\rm MBPT}$	Composition
26	58	$2s^22p^4(^1D)3d$	$^2P_{1/2}$	7074200	7073075	7073108	4.04E−14	4.10E−14	61.4 (58) 32.4 (42) 4.90 (52)
26	59	$2s2p^5(^3P)3s$	$^4P_{5/2}$	7185800	7161578	7162287	1.71E−11	1.74E−11	98.7 (59)
26	60	$2s^22p^4(^1S)3d$	$^2D_{5/2}$	7166400	7164696	7165527	9.51E−13	9.50E−13	78.9 (60)
26	61	$2s^22p^4(^1S)3d$	$^2D_{3/2}$	7184300	7183174	7183610	7.71E−14	7.89E−14	69.8 (61) 12.6 (46) 6.63 (43)
26	62	$2s2p^5(^3P)3s$	$^4P_{3/2}$	7197800	7197130	7197483	1.83E−12	1.81E−12	67.1 (62) 30.7 (64) 0.903 (77)
26	63	$2s2p^5(^3P)3s$	$^4P_{1/2}$	7224600	7243238	7243764	2.59E−12	2.56E−12	81.3 (63)
26	64	$2s2p^5(^3P)3s$	$^2P_{3/2}$	7250900	7250219	7250017	1.28E−12	1.32E−12	67.7 (64) 29.5 (62) 1.68 (77)
26	65	$2s2p^5(^3P)3s$	$^2P_{1/2}$	···	7304198	7303972	7.01E−13	7.14E−13	79.3 (65)
26	66	$2s2p^5(^3P)3p$	$^4S_{3/2}$	···	7395295	7396147	1.47E−11	1.49E−11	77.9 (66)
26	67	$2s2p^5(^3P)3p$	$^4D_{5/2}$	···	7422724	7423214	1.29E−12	1.29E−12	57.1 (67) 24.6 (70) 17.6 (74)
26	68	$2s2p^5(^3P)3p$	$^4D_{7/2}$	···	7431839	7432497	1.99E−11	2.03E−11	99.4 (68)
26	69	$2s2p^5(^3P)3p$	$^4D_{3/2}$	7464400	7447995	7448495	8.06E−13	8.04E−13	41.6 (69) 26.9 (72) 11.3 (79)
26	70	$2s2p^5(^3P)3p$	$^2D_{5/2}$	7477200	7460866	7461183	5.93E−13	5.99E−13	50.5 (70) 48.1 (74) 0.665 (67)
26	71	$2s2p^5(^3P)3p$	$^4D_{1/2}$	···	7474455	7474858	1.76E−12	1.71E−12	46.3 (71) 33.2 (76) 16.8 (73)
26	72	$2s2p^5(^3P)3p$	$^2P_{3/2}$	7487800	7487268	7487633	3.83E−13	3.88E−13	60.9 (72) 35.9 (69) 1.88 (86)
26	73	$2s2p^5(^3P)3p$	$^2P_{1/2}$	7508100	7503954	7503646	2.66E−13	2.68E−13	50.3 (73) 24.1 (80) 9.81 (76)
26	74	$2s2p^5(^3P)3p$	$^4P_{5/2}$	7508100	7507510	7507960	8.20E−13	8.30E−13	39.9 (67) 32.6 (74) 23.6 (70)
26	75	$2s2p^5(^3P)3p$	$^4P_{3/2}$	7529900	7512026	7512395	8.10E−13	8.15E−13	44.3 (75) 42.2 (79) 8.98 (66)
26	76	$2s2p^5(^3P)3p$	$^4P_{1/2}$	···	7517157	7517610	9.29E−12	9.98E−12	52.7 (76) 44.9 (71) 0.652 (73)
26	77	$2s2p^5(^1P)3s$	$^2P_{3/2}$	···	7520103	7519819	9.71E−13	9.86E−13	96.1 (77)
26	78	$2s2p^5(^1P)3s$	$^2P_{1/2}$	···	7526471	7526062	1.98E−12	2.01E−12	93.6 (78)
26	79	$2s2p^5(^3P)3p$	$^2D_{3/2}$	7567000	7557262	7557691	5.76E−13	5.84E−13	43.7 (79) 23.9 (75) 17.8 (69)
26	80	$2s2p^5(^3P)3p$	$^2S_{1/2}$	7599400	7577251	7575702	2.32E−13	2.38E−13	55.9 (80) 30.0 (73) 7.11 (94)
26	81	$2s2p^5(^3P)3d$	$^4P_{1/2}$	···	7722864	7723443	1.50E−11	1.54E−11	97.1 (81)
26	82	$2s2p^5(^3P)3d$	$^4P_{3/2}$	···	7731650	7732195	1.17E−11	1.20E−11	87.7 (82)
26	83	$2s2p^5(^3P)3d$	$^4F_{9/2}$	···	7739704	7740052	2.54E−11	2.63E−11	99.9 (83)
26	84	$2s2p^5(^3P)3d$	$^4P_{5/2}$	···	7746896	7747351	1.85E−11	1.90E−11	61.6 (84) 30.3 (97) 7.20 (87)
26	85	$2s2p^5(^3P)3d$	$^4F_{7/2}$	···	7750799	7751071	2.36E−11	2.44E−11	75.6 (85)
26	86	$2s2p^5(^1P)3p$	$^2D_{3/2}$	7763400	7762208	7761801	5.96E−13	6.02E−13	89.9 (86)
26	87	$2s2p^5(^3P)3d$	$^4F_{5/2}$	···	7771208	7771411	2.08E−11	2.14E−11	54.0 (87) 17.5 (95) 13.7 (84)
26	88	$2s2p^5(^3P)3d$	$^2F_{7/2}$	···	7784767	7784728	1.95E−11	2.01E−11	54.8 (88) 43.7 (96) 1.11 (85)
26	89	$2s2p^5(^1P)3p$	$^2D_{5/2}$	7783900	7785252	7784846	9.59E−13	9.71E−13	95.9 (89)
26	90	$2s2p^5(^3P)3d$	$^4F_{3/2}$	···	7788857	7789007	1.54E−12	1.52E−12	51.0 (90) 22.7 (98) 18.0 (99)
26	91	$2s2p^5(^1P)3p$	$^2P_{1/2}$	7786000	7794271	7793992	6.17E−13	6.22E−13	94.6 (91)
26	92	$2s2p^5(^1P)3p$	$^2P_{3/2}$	7794400	7804850	7804611	8.18E−13	8.24E−13	90.9 (92)
26	93	$2s2p^5(^3P)3d$	$^4D_{1/2}$	···	7817935	7817987	4.28E−13	4.21E−13	89.4 (93)
26	94	$2s2p^5(^1P)3p$	$^2S_{1/2}$	···	7824952	7821304	6.87E−12	6.90E−12	79.9 (94)
26	95	$2s2p^5(^3P)3d$	$^2D_{5/2}$	···	7828946	7828832	1.71E−11	1.75E−11	40.7 (95) 30.7 (101) 11.5 (84)
26	96	$2s2p^5(^3P)3d$	$^4D_{7/2}$	···	7830553	7830584	1.73E−11	1.78E−11	38.6 (88) 37.1 (96) 21.7 (85)
26	97	$2s2p^5(^3P)3d$	$^4D_{5/2}$	···	7830898	7830978	1.70E−11	1.76E−11	40.5 (97) 19.8 (87) 19.4 (95)
26	98	$2s2p^5(^3P)3d$	$^4D_{3/2}$	···	7839025	7839148	9.06E−12	1.27E−11	58.5 (98) 21.8 (99) 8.12 (90)
26	99	$2s2p^5(^3P)3d$	$^2D_{3/2}$	···	7843195	7842994	3.45E−13	3.42E−13	39.1 (99) 36.7(90) 18.2 (102)
26	100	$2s2p^5(^3P)3d$	$^2P_{1/2}$	···	7866302	7865441	8.26E−14	8.46E−14	84.7 (100)
26	101	$2s2p^5(^3P)3d$	$^2F_{5/2}$	···	7881249	7881189	1.69E−11	1.75E−11	47.6 (101) 20.0 (95) 17.2 (97)
26	102	$2s2p^5(^3P)3d$	$^2P_{3/2}$	···	7924316	7923382	7.14E−14	7.27E−14	72.9 (102)
26	103	$2s2p^5(^1P)3d$	$^2F_{5/2}$	···	8099131	8098151	6.11E−12	6.32E−12	93.0 (103)
26	104	$2s2p^5(^1P)3d$	$^2F_{7/2}$	···	8100003	8099049	6.21E−12	6.43E−12	96.7 (104)
26	105	$2s2p^5(^1P)3d$	$^2P_{3/2}$	···	8109297	8108029	7.50E−14	7.61E−14	90.5 (105)
26	106	$2s2p^5(^1P)3d$	$^2P_{1/2}$	···	8117127	8115631	5.46E−14	5.57E−14	87.2 (106)
26	107	$2s2p^5(^1P)3d$	$^2D_{5/2}$	···	8128204	8127479	7.12E−12	7.33E−12	94.5 (107)
26	108	$2s2p^5(^1P)3d$	$^2D_{3/2}$	···	8128827	8128004	5.54E−13	6.04E−13	92.4 (108)
26	109	$2s^22p^4(^3P)4s$	$^4P_{5/2}$	···	8417656	8418381	2.21E−12	2.20E−12	90.7 (109)
26	110	$2p^63s$	$^2S_{1/2}$	···	8418105	8415573	5.38E−12	5.56E−12	95.6 (110)
26	111	$2s^22p^4(^3P)4s$	$^2P_{3/2}$	8428200	8426924	8427554	9.35E−13	9.36E−13	70.7 (111) 18.9 (113) 10.2 (122)
26	112	$2s^22p^4(^3P)4s$	$^4P_{1/2}$	···	8495236	8495489	1.80E−12	1.78E−12	73.1 (112)
26	113	$2s^22p^4(^3P)4s$	$^4P_{3/2}$	8517200	8508688	8509349	1.61E−12	1.61E−12	79.7 (113)

Table 1
(Continued)

Z	Key	Configuration	Term	$E_{\rm NIST}$	$E_{\rm MCDHF}$	$E_{\rm MBPT}$	$\tau_{\rm MCDHF}$	$\tau_{\rm MBPT}$	Composition
26	114	$2s^22p^4(^3P)4s$	$^2P_{1/2}$	⋯	8516141	8516681	8.30E−13	8.35E−13	84.0 (114)
26	115	$2s^22p^4(^3P)4p$	$^4P_{3/2}$	⋯	8519369	8519796	2.38E−12	2.37E−12	50.6 (115) 21.4 (127) 8.45 (124)
26	116	$2s^22p^4(^3P)4p$	$^4P_{5/2}$	⋯	8519501	8519969	2.39E−12	2.38E−12	55.3 (116) 31.8 (126) 5.99 (144)
26	117	$2s^22p^4(^3P)4p$	$^4D_{7/2}$	⋯	8530427	8531072	2.46E−12	2.45E−12	90.2 (117)
26	118	$2s^22p^4(^3P)4p$	$^2D_{5/2}$	⋯	8531020	8531541	2.37E−12	2.38E−12	66.8 (118) 17.6 (116) 8.02 (141)
26	119	$2s^22p^4(^3P)4p$	$^2S_{1/2}$	⋯	8534332	8534644	2.38E−12	2.41E−12	39.7 (119) 23.6 (129) 19.8 (125)
26	120	$2s^22p^4(^3P)4p$	$^2P_{3/2}$	⋯	8558366	8558164	2.56E−12	2.63E−12	39.5 (120) 26.5 (127) 17.9 (128)
26	121	$2s^22p^4(^1D)4s$	$^2D_{5/2}$	8591100	8589712	8590170	1.23E−12	1.22E−12	90.4 (121)
26	122	$2s^22p^4(^1D)4s$	$^2D_{3/2}$	8593000	8590974	8591417	1.26E−12	1.25E−12	89.5 (122)
26	123	$2s^22p^4(^3P)4p$	$^4D_{1/2}$	⋯	8596694	8596730	2.32E−12	2.34E−12	50.1 (123) 18.8 (183) 15.6 (125)
26	124	$2s^22p^4(^3P)4p$	$^4D_{3/2}$	⋯	8606168	8606402	2.41E−12	2.41E−12	60.2 (124) 16.2 (115) 14.4 (184)
26	125	$2s^22p^4(^3P)4p$	$^4P_{1/2}$	⋯	8606930	8607314	2.34E−12	2.33E−12	55.0 (125) 23.2 (123) 15.1 (119)
26	126	$2s^22p^4(^3P)4p$	$^4D_{5/2}$	⋯	8618780	8619306	2.45E−12	2.44E−12	58.8 (126) 21.5 (116) 19.4 (118)
26	127	$2s^22p^4(^3P)4p$	$^4S_{3/2}$	⋯	8622454	8622553	2.39E−12	2.41E−12	30.7 (120) 24.8 (127) 19.2 (115)
26	128	$2s^22p^4(^3P)4p$	$^2D_{3/2}$	⋯	8626850	8627172	2.36E−12	2.42E−12	70.7 (128) 12.6 (127) 9.14 (120)
26	129	$2s^22p^4(^3P)4p$	$^2P_{1/2}$	⋯	8632048	8631870	2.36E−12	2.37E−12	41.7 (129) 29.0 (119) 13.9 (123)
26	130	$2s^22p^4(^3P)4d$	$^4D_{7/2}$	⋯	8644406	8645054	1.36E−12	1.35E−12	65.6 (130) 24.4 (160) 7.96 (179)
26	131	$2s^22p^4(^3P)4d$	$^4D_{5/2}$	⋯	8644690	8645332	1.36E−12	1.36E−12	62.2 (131) 14.6 (163) 12.1 (158)
26	132	$2s^22p^4(^3P)4d$	$^4D_{3/2}$	⋯	8647125	8647783	1.31E−12	1.30E−12	47.6 (132) 30.9 (161) 6.40 (181)
26	133	$2s^22p^4(^3P)4d$	$^4P_{1/2}$	⋯	8650769	8651447	1.21E−12	1.22E−12	39.6 (133) 28.8 (159) 19.6 (137)
26	134	$2s^22p^4(^3P)4d$	$^4F_{9/2}$	⋯	8651454	8652279	1.37E−12	1.37E−12	90.0 (134)
26	135	$2p^63p$	$^2P_{1/2}$	⋯	8651848	8649313	5.00E−13	5.10E−13	95.3 (135)
26	136	$2s^22p^4(^3P)4d$	$^2F_{7/2}$	⋯	8655791	8656533	1.39E−12	1.39E−12	68.3 (136) 19.3 (160) 10.6 (174)
26	137	$2s^22p^4(^3P)4d$	$^2P_{1/2}$	⋯	8664235	8664800	4.12E−13	4.24E−13	43.1 (133) 41.2 (137) 9.41 (177)
26	138	$2s^22p^4(^3P)4d$	$^2D_{3/2}$	8676000	8673684	8673963	2.23E−13	2.32E−13	32.6 (138) 31.9 (161) 21.6 (165)
26	139	$2p^63p$	$^2P_{3/2}$	⋯	8675769	8673205	4.99E−13	5.09E−13	96.0 (139)
26	140	$2s^22p^4(^3P)4d$	$^2D_{5/2}$	8676000	8675882	8676101	2.05E−13	2.13E−13	42.0 (140) 22.7 (164) 17.1 (163)
26	141	$2s^22p^4(^1D)4p$	$^2F_{5/2}$	⋯	8689859	8690229	2.31E−12	2.30E−12	81.5 (141)
26	142	$2s^22p^4(^1D)4p$	$^2F_{7/2}$	⋯	8698580	8698933	2.42E−12	2.41E−12	90.1 (142)
26	143	$2s^22p^4(^1D)4p$	$^2P_{3/2}$	⋯	8701961	8701813	2.51E−12	2.54E−12	63.4 (143) 29.0 (145) 4.86 (127)
26	144	$2s^22p^4(^1D)4p$	$^2D_{5/2}$	⋯	8707674	8708250	2.49E−12	2.52E−12	83.1 (144)
26	145	$2s^22p^4(^1D)4p$	$^2D_{3/2}$	⋯	8708223	8707788	2.50E−12	2.52E−12	59.5 (145) 24.6 (143) 11.1 (120)
26	146	$2s^22p^4(^3P)4f$	$^4F_{7/2}$	⋯	8713450	8714242	6.28E−13	6.34E−13	48.7 (146) 20.7 (170) 11.1 (151)
26	147	$2s^22p^4(^3P)4f$	$^4F_{9/2}$	⋯	8713503	8714301	6.28E−13	6.33E−13	58.4 (147) 29.3 (169) 8.79 (194)
26	148	$2s^22p^4(^3P)4f$	$^4F_{5/2}$	⋯	8714321	8715131	6.24E−13	6.30E−13	44.9 (148) 15.2 (153) 14.4 (171)
26	149	$2s^22p^4(^3P)4f$	$^2G_{9/2}$	⋯	8715646	8716335	6.51E−13	6.59E−13	70.7 (149) 18.0 (169) 10.1 (185)
26	150	$2s^22p^4(^3P)4f$	$^4G_{11/2}$	⋯	8715843	8716581	6.47E−13	6.55E−13	89.8 (150)
26	151	$2s^22p^4(^3P)4f$	$^2F_{7/2}$	⋯	8715898	8716598	6.54E−13	6.62E−13	47.9 (151) 15.6 (173) 14.3 (167)
26	152	$2s^22p^4(^3P)4f$	$^4D_{3/2}$	⋯	8716491	8717340	6.20E−13	6.26E−13	35.7 (152) 34.1 (168) 20.1 (155)
26	153	$2s^22p^4(^3P)4f$	$^4D_{5/2}$	⋯	8718274	8719028	6.47E−13	6.55E−13	33.3 (153) 31.4 (171) 20.4 (172)
26	154	$2s^22p^4(^3P)4f$	$^4D_{1/2}$	⋯	8719110	8719978	6.22E−13	6.29E−13	89.2 (154)
26	155	$2s^22p^4(^3P)4f$	$^2D_{3/2}$	⋯	8720325	8721122	6.36E−13	6.44E−13	52.0 (155) 36.8 (152) 10.4 (188)
26	156	$2s^22p^4(^3P)4d$	$^4F_{3/2}$	8727500	8726056	8726357	1.05E−12	1.04E−12	55.5 (156) 17.8 (198) 14.7 (132)
26	157	$2s^22p^4(^1D)4p$	$^2P_{1/2}$	⋯	8726779	8725481	2.74E−12	2.80E−12	78.3 (157)
26	158	$2s^22p^4(^3P)4d$	$^4F_{5/2}$	8727500	8728437	8728833	1.07E−12	1.05E−12	44.7 (158) 21.5 (131) 15.5 (196)
26	159	$2s^22p^4(^3P)4d$	$^4D_{1/2}$	⋯	8734706	8735195	8.42E−13	8.57E−13	67.0 (159) 21.9 (137) 7.90 (133)
26	160	$2s^22p^4(^3P)4d$	$^4F_{7/2}$	⋯	8738876	8739571	1.37E−12	1.37E−12	51.3 (160) 28.2 (130) 20.0 (136)
26	161	$2s^22p^4(^3P)4d$	$^4P_{3/2}$	⋯	8742234	8742761	5.63E−13	5.87E−13	30.1 (132) 23.9 (161) 19.6 (156)
26	162	$2s^22p^4(^1S)4s$	$^2S_{1/2}$	⋯	8746200	8742978	1.10E−12	1.09E−12	78.1 (162)
26	163	$2s^22p^4(^3P)4d$	$^4P_{5/2}$	⋯	8746546	8747289	1.13E−12	1.13E−12	44.8 (163) 30.4 (164) 16.1 (158)
26	164	$2s^22p^4(^3P)4d$	$^2F_{5/2}$	8756600	8755056	8755213	2.00E−13	2.13E−13	43.8 (140) 37.2 (164) 12.8 (158)
26	165	$2s^22p^4(^3P)4d$	$^2P_{3/2}$	8759900	8758783	8758888	2.74E−13	2.87E−13	50.7 (165) 28.0 (138) 9.94 (156)
26	166	$2s^22p^4(^3P)4f$	$^4G_{5/2}$	⋯	8790618	8790963	6.38E−13	6.45E−13	41.4 (166) 19.7 (199) 13.1 (172)
26	167	$2s^22p^4(^3P)4f$	$^2G_{7/2}$	⋯	8791487	8791832	6.41E−13	6.49E−13	20.8 (167) 19.7 (200) 18.9 (173)
26	168	$2s^22p^4(^3P)4f$	$^4F_{3/2}$	⋯	8803208	8804004	6.23E−13	6.28E−13	62.6 (168) 18.8 (155) 18.4 (152)
26	169	$2s^22p^4(^3P)4f$	$^4G_{9/2}$	⋯	8803888	8804630	6.37E−13	6.44E−13	47.3 (169) 35.2 (147) 17.4 (149)

Table 1
(Continued)

Z	Key	Configuration	Term	$E_{\rm NIST}$	$E_{\rm MCDHF}$	$E_{\rm MBPT}$	$\tau_{\rm MCDHF}$	$\tau_{\rm MBPT}$	Composition
26	170	$2s^22p^4(^3P)4f$	$^4G_{7/2}$	···	8803915	8804595	6.50E−13	6.58E−13	38.2 (170) 28.5 (151) 25.8 (167)
26	171	$2s^22p^4(^3P)4f$	$^2F_{5/2}$	···	8804662	8805423	6.34E−13	6.41E−13	34.7 (153) 31.4 (171) 28.9 (148)
26	172	$2s^22p^4(^3P)4f$	$^2D_{5/2}$	···	8807560	8808274	6.51E−13	6.59E−13	47.7 (172) 40.0 (166) 6.83 (171)
26	173	$2s^22p^4(^3P)4f$	$^4D_{7/2}$	···	8807872	8808643	6.38E−13	6.46E−13	51.1 (173) 29.0 (167) 15.5 (170)
26	174	$2s^22p^4(^1D)4d$	$^2G_{7/2}$	···	8816235	8816794	1.37E−12	1.37E−12	87.5 (174)
26	175	$2s^22p^4(^1D)4d$	$^2G_{9/2}$	···	8817606	8818169	1.37E−12	1.36E−12	90.0 (175)
26	176	$2s^22p^4(^1D)4d$	$^2D_{5/2}$	8829200	8825756	8826291	9.17E−13	8.77E−13	55.8 (176) 36.7 (180) 2.99 (140)
26	177	$2s^22p^4(^1D)4d$	$^2S_{1/2}$	8829200	8826721	8826911	1.58E−13	1.61E−13	77.9(177)
26	178	$2s^22p^4(^1D)4d$	$^2P_{3/2}$	8829200	8828677	8828638	1.62E−13	1.69E−13	87.7 (178)
26	179	$2s^22p^4(^1D)4d$	$^2F_{7/2}$	···	8829753	8830436	1.39E−12	1.41E−12	89.4 (179)
26	180	$2s^22p^4(^1D)4d$	$^2F_{5/2}$	8829200	8831794	8832086	2.79E−13	3.04E−13	52.7 (180) 35.6 (176) 5.09 (140)
26	181	$2s^22p^4(^1D)4d$	$^2D_{3/2}$	8843900	8841152	8841076	1.55E−13	1.63E−13	82.5 (181)
26	182	$2s^22p^4(^1D)4d$	$^2P_{1/2}$	8843900	8844793	8844467	1.10E−13	1.14E−13	71.0 (182) 16.9 (137) 10.9 (177)
26	183	$2s^22p^4(^1S)4p$	$^2P_{1/2}$	···	8856013	8852665	2.12E−12	2.15E−12	77.0 (183)
26	184	$2s^22p^4(^1S)4p$	$^2P_{3/2}$	···	8858407	8855268	2.23E−12	2.23E−12	79.7 (184)
26	185	$2s^22p^4(^1D)4f$	$^2H_{9/2}$	···	8880153	8880639	6.47E−13	6.55E−13	89.6 (185)
26	186	$2s^22p^4(^1D)4f$	$^2H_{11/2}$	···	8880875	8881359	6.48E−13	6.55E−13	89.8 (186)
26	187	$2s^22p^4(^1D)4f$	$^2P_{1/2}$	···	8881342	8882006	5.94E−13	5.98E−13	88.9 (187)
26	188	$2s^22p^4(^1D)4f$	$^2P_{3/2}$	···	8881963	8882634	5.96E−13	6.00E−13	87.1 (188)
26	189	$2s^22p^4(^1D)4f$	$^2D_{5/2}$	···	8885492	8886201	6.14E−13	6.19E−13	89.1 (189)
26	190	$2s^22p^4(^1D)4f$	$^2D_{3/2}$	···	8885641	8886297	6.27E−13	6.34E−13	87.9 (190)
26	191	$2s^22p^4(^1D)4f$	$^2G_{7/2}$	···	8887996	8888604	6.47E−13	6.56E−13	84.2 (191)
26	192	$2s^22p^4(^1D)4f$	$^2F_{5/2}$	···	8888465	8889083	6.40E−13	6.48E−13	89.6 (192)
26	193	$2s^22p^4(^1D)4f$	$^2F_{7/2}$	···	8888653	8889304	6.31E−13	6.38E−13	84.1 (193)
26	194	$2s^22p^4(^1D)4f$	$^2G_{9/2}$	···	8888781	8889387	6.48E−13	6.57E−13	90.9 (194)
26	195	$2p^63d$	$^2D_{3/2}$	···	8979016	8975356	1.61E−12	1.23E−12	89.4 (195)
26	196	$2s^22p^4(^1S)4d$	$^2D_{5/2}$	···	8979073	8975468	8.99E−13	9.71E−13	59.4 (196) 24.9 (197) 4.24 (164)
26	197	$2p^63d$	$^2D_{5/2}$	···	8984723	8982100	4.06E−12	3.52E−12	74.5 (197)
26	198	$2s^22p^4(^1S)4d$	$^2D_{3/2}$	8989200	8985678	8982974	2.79E−13	3.19E−13	70.0 (198) 9.72 (195) 7.92 (156)
26	199	$2s^22p^4(^1S)4f$	$^2F_{5/2}$	···	9041025	9038310	6.46E−13	6.56E−13	79.2 (199)
26	200	$2s^22p^4(^1S)4f$	$^2F_{7/2}$	···	9041604	9038912	6.39E−13	6.48E−13	79.2 (200)

Note. Subscripts MCDHF and MBPT represent the present calculations; the subscript NIST represents values from Kramida et al. (2016). The NIST identification of $2s^22p^4(^1S)4d\ ^2D_{1/2}$ for Zn XXII is a misprint (Sugar & Musgrove 1995), and is replaced by $2s^22p^4(^1S)4d\ ^2D_{3/2}$.

(This table is available in its entirety in machine-readable form.)

electron-impact excitation for levels with n up to 4 for F-like ions from Ne^+ to Kr^{27+} where the target structures were calculated using the AUTOSTRUCTURE code (Badnell 1986). Nahar (2006) performed large scale relativistic Breit-Pauli calculations for energy levels and transition rates of 1174 levels in Fe XVIII. Among the above calculations, values from Gu (2005b, 2007) are the most accurate ones but lack transition rates, while energy levels calculated by Jonauskas et al. (2004), Witthoeft et al. (2006, 2007) and Nahar (2006) differ from observations by up to 0.7%, 1% and 1%, respectively. This is not sufficiently accurate to meet the requirements of the new instruments for X-ray astronomy (Kallman & Palmeri 2007). There is therefore a clear demand for more accurate and complete energy levels and transition rates for F-like ions.

In the present paper, we continue our effort to produce an accurate and consistent data set of energy levels and transition characteristic for ions of astrophysics interest (Wang et al. 2014, 2015, 2016; Si et al. 2016) by providing energy levels and transition rates for F-like ions with $Z = 24$–30. Using two state-of-the-art approaches, the MCDHF and the second-order many-body perturbation theory (MBPT), we present the 200 lowest bound energy levels arising from $1s^22s^22p^5$, $1s^22s2p^6$, $1s^22s^22p^43l$, $1s^22s2p^53l$, $1s^22p^63l$, and $1s^22s^22p^44l$ configurations, as well as multipole transition rates (electric dipole, quadrupole, and octopole, as well as magnetic dipole, and quadrupole) and the resulting lifetimes. For the MCDHF calculation we use the latest version of the GRASP2K code (Jönsson et al. 2013b), while the MBPT calculation is performed using the Flexible Atomic Code (FAC; Gu 2008). As we will show, the two sets of theoretical values are in excellent agreement, and the present work represents a significant extension of accurate energy levels and transition rates over previous theoretical work on F-like ions, especially for the $n = 3$ and $n = 4$ states.

2. CALCULATION

2.1. MCDHF

The starting point of the MCDHF approach (Grant 2007) implemented in the GRASP2K package (Jönsson et al. 2013b)

Table 2
The NIST Kramida et al. (2016) Level Identifications That Differ from the Present Ones in Table 1

		PRESENT		NIST				PRESENT		NIST	
Z	Key	Configuration	Term	Configuration	Term	Z	Key	Configuration	Term	Configuration	Term
24	5	$2s^22p^4(^3P)3s$	$^2P_{3/2}$	$2s^22p^4(^3P)3s$	$^4P_{3/2}$	24	7	$2s^22p^4(^3P)3s$	$^4P_{3/2}$	$2s^22p^4(^3P)3s$	$^2P_{3/2}$
25	5	$2s^22p^4(^3P)3s$	$^2P_{3/2}$	$2s^22p^4(^3P)3s$	$^4P_{3/2}$	25	7	$2s^22p^4(^3P)3s$	$^4P_{3/2}$	$2s^22p^4(^3P)3s$	$^2P_{3/2}$
25	41	$2s^22p^4(^3P)3d$	$^2F_{5/2}$	$2s^22p^4(^3P)3d$	$^4F_{5/2}$	25	44	$2s^22p^4(^3P)3d$	$^4F_{5/2}$	$2s^22p^4(^3P)3d$	$^4P_{5/2}$
25	47	$2s^22p^4(^3P)3d$	$^4P_{5/2}$	$2s^22p^4(^3P)3d$	$^2F_{5/2}$	26	42	$2s^22p^4(^3P)3d$	$^2P_{1/2}$	$2s^22p^4(^3P)3d$	$^4D_{1/2}$
26	44	$2s^22p^4(^3P)3d$	$^4F_{5/2}$	$2s^22p^4(3^P)3d$	$^4P_{5/2}$	26	46	$2s^22p^4(^3P)3d$	$^2D_{3/2}$	$2s^22p^4(^3P)3d$	$^4D_{3/2}$
27	75	$2s2p^5(^3P)3p$	$^2D_{3/2}$	$2s2p^5(^3P)3p$	$^4P_{3/2}$	27	79	$2s2p^5(^3P)3p$	$^4P_{3/2}$	$2s2p^5(^3P)3p$	$^2D_{3/2}$
28	17	$2s^22p^4(^3P)3p$	$^4S_{3/2}$	$2s^22p^4(^3P)3p$	$^4D_{3/2}$	28	44	$2s^22p^4(^3P)3d$	$^2P_{1/2}$	$2s^22p^4(^3P)3d$	$^4D_{1/2}$
28	46	$2s^22p^4(^3P)3d$	$^2D_{3/2}$	$2s^22p^4(^3P)3d$	$^4D_{3/2}$	28	70	$2s2p^5(^3P)3p$	$^4P_{5/2}$	$2s2p^5(^3P)3p$	$^2D_{5/2}$
28	76	$2s2p^5(^3P)3p$	$^2D_{3/2}$	$2s2p^5(^3P)3p$	$^4P_{3/2}$	28	79	$2s2p^5(^3P)3p$	$^4P_{3/2}$	$2s2p^5(^3P)3p$	$^2D_{3/2}$
29	17	$2s^22p^4(^3P)3p$	$^4S_{3/2}$	$2s^22p^4(^3P)3p$	$^4D_{3/2}$	29	37	$2s^22p^4(^3P)3d$	$^2P_{1/2}$	$2s^22p^4(^3P)3d$	$^4P_{1/2}$
29	39	$2s^22p^4(^3P)3d$	$^2D_{5/2}$	$2s^22p^4(^3P)3d$	$^2F_{5/2}$	29	46	$2s^22p^4(^3P)3d$	$^2D_{3/2}$	$2s^22p^4(^3P)3d$	$^4D_{3/2}$
29	49	$2s^22p^4(^3P)3d$	$^2F_{5/2}$	$2s^22p^4(^3P)3d$	$^2D_{5/2}$	29	56	$2s^22p^4(^1D)3d$	$^2F_{5/2}$	$2s^22p^4(^1D)3d$	$^2D_{5/2}$
29	69	$2s2p^5(^3P)3p$	$^2P_{3/2}$	$2s2p^5(^3P)3p$	$^4D_{3/2}$	29	70	$2s2p^5(^3P)3p$	$^4P_{5/2}$	$2s2p^5(^3P)3p$	$^2D_{5/2}$
29	72	$2s2p^5(^3P)3p$	$^4D_{3/2}$	$2s2p^5(^3P)3p$	$^2P_{3/2}$	29	75	$2s2p^5(^3P)3p$	$^2D_{5/2}$	$2s2p^5(^3P)3p$	$^4P_{5/2}$
29	76	$2s2p^5(^3P)3p$	$^2D_{3/2}$	$2s2p^5(^3P)3p$	$^4P_{3/2}$	29	79	$2s2p^5(^3P)3p$	$^4P_{3/2}$	$2s2p^5(^3P)3p$	$^2D_{3/2}$
30	37	$2s^22p^4(^3P)3d$	$^2P_{1/2}$	$2s^22p^4(^3P)3d$	$^4P_{1/2}$	30	39	$2s^22p^4(^3P)3d$	$^2D_{5/2}$	$2s^22p^4(^3P)3d$	$^4P_{5/2}$
30	46	$2s^22p^4(^3P)3d$	$^2D_{3/2}$	$2s^22p^4(^3P)3d$	$^4D_{3/2}$	30	49	$2s^22p^4(^3P)3d$	$^2F_{5/2}$	$2s^22p^4(^3P)3d$	$^2P_{5/2}$
30	56	$2s^22p^4(^1D)3d$	$^2F_{5/2}$	$2s^22p^4(^1D)3d$	$^2P_{5/2}$	30	69	$2s2p^5(^3P)3p$	$^2P_{3/2}$	$2s2p^5(^3P)3p$	$^4D_{3/2}$
30	72	$2s2p^5(^3P)3p$	$^4D_{3/2}$	$2s2p^5(^3P)3p$	$^2P_{3/2}$	30	76	$2s2p^5(^3P)3p$	$^2D_{3/2}$	$2s2p^5(^3P)3p$	$^4D_{3/2}$

is the (Dirac–Coulomb) Hamiltonian

$$\hat{H}_{\rm DC} = \sum_{i=1}^{N}[h_d(i) + V_i^N] + \sum_{i<j}^{N}\frac{1}{r_{ij}}, \quad (1)$$

where $h_d(i)$ is the Dirac Hamiltonian for one free electron, V_i^N is the monopole part of the electron-nucleus Coulomb interaction. The atomic state functions are given by expansions of configuration state functions (CSFs)

$$\Psi_\alpha(PJM) = \sum_{r=1}^{n_c} c_r(\alpha)\Phi(\gamma_r PJM). \quad (2)$$

In the above expression P is the parity, J and M are the angular momentum quantum numbers, and γ denotes other appropriate labeling of the CSF r, such as orbital occupancy and coupling scheme. n_c and $c_r(\alpha)$ are the number of CSFs and configuration mixing coefficients, respectively. The CSFs are built from anti-symmetrized and coupled products of one-electron Dirac orbitals. The radial parts of the Dirac orbitals are determined in the extended optimal level scheme, and the expansion coefficients $c_r(\alpha)$ are obtained in the relativistic self-consistent field (RSCF) procedure (Dyall et al. 1989). The Breit interaction

$$H_{\rm Breit} = \sum_{i<j}^{N} B_{ij} = -\sum_{i<j}^{N}\frac{1}{2r_{ij}}\left[\alpha_i\cdot\alpha_j + \frac{(\alpha_i\cdot r_{ij})(\alpha_j\cdot r_{ij})}{r_{ij}^2}\right] \quad (3)$$

and QED (vacuum polarization and self-energy) corrections can be included in subsequent configuration interaction (RCI) calculations (McKenzie et al. 1980).

The CSF expansions are obtained with the restricted active space method (Brage & Fischer 1993; Sturesson et al. 2007), which is to excite electrons from the occupied orbitals in the multireference (MR) configurations to unoccupied orbitals in an active set. In the present work, the $1s^22s^22p^5$, $1s^22s2p^6$, $1s^22s^22p^43l$, $1s^22s2p^53l$, $1s^22p^63l$, and $1s^22s^22p^44l$ configurations are chosen as MR configurations. Subsequently, the CSF expansions are generated by single and double (SD) substitutions of the orbitals in the MR with the orbitals in active sets with $n \leqslant 7$, $l \leqslant 4$. With this approach, the valence–valence and core–valence correlations are taken into account. The resulting level energies and lifetimes are generally converged to within 0.01% and 3%, respectively. The final expansion contains 1923543 even and 1976470 odd CSFs distributed over different J^π symmetries.

2.2. MBPT

In the MBPT method (Lindgren 1974; Safronova et al. 1996) implemented by Gu et al. (2006), the (Dirac–Coulomb–Breit) Hamiltonian can be written as

$$\hat{H}_{\rm DCB} = \sum_{i}^{N}\left[h_d(i) - \frac{Z}{r_i}\right] + \sum_{i<j}^{N}\left(\frac{1}{r_{ij}} + B_{ij}\right). \quad (4)$$

The $H_{\rm DCB}$ is divided into a model Hamiltonian H_0 and a perturbation V,

$$H_0 = \sum_i [h_d(i) + U(r_i)], \quad (5)$$

$$V = -\sum_i\left[\frac{Z}{r_i} + U(r_i)\right] + \sum_{i<j}^{N}\left(\frac{1}{r_{ij}} + B_{ij}\right). \quad (6)$$

Through a RSCF calculation, $U(r_i)$ which is approximated as a local central potential, can be derived. After $U(r_i)$ is determined, the eigenfunctions Φ_r of H_0 can be constructed from one-electron orbitals. A portion of Φ_r defines the model space M and what remains is in the orthogonal space N. In the M space, a non-Hermitian effective Hamiltonian $H_{\rm eff}$ whose eigenvalues are the eigenenergies of $H_{\rm DCB}$ can be constructed

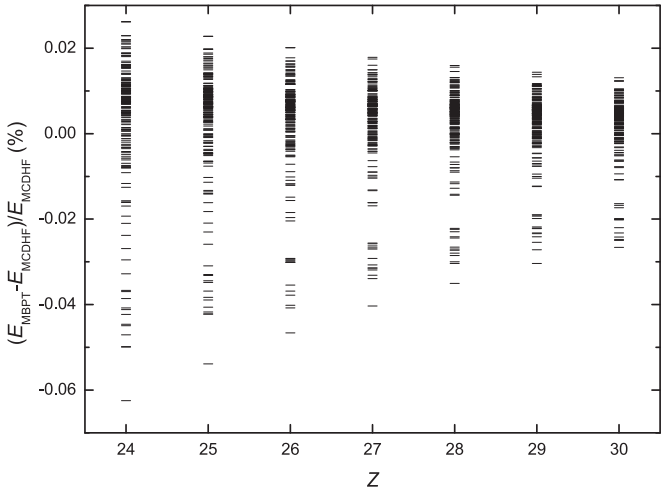

Figure 1. Comparison of the present MBPT and MCDHF excitation energies of $n = 3$ and $n = 4$ configurations.

with perturbation expansion. The eigenenergies of H_{DCB} in second-order are obtained through solving the generalized eigenvalue problem of the first order H_{eff}. In this way, the CI effects within the M space are exactly included, and CI effects between M and N are taken into account to second-order. Finally, several small corrections to the Hamiltonian, such as QED are also included.

In the present MBPT calculation, the configurations in the model space M are the same as the MR configurations in the MCDHF calculation, while all the possible configurations that are generated by SD excitations from the M space are contained in the N space. The maximum n values for SD excitations are 125 and 65, while the maximum l values are 20.

3. RESULTS

3.1. Energy Levels

In Table 1, we present the lowest 200 excitation energy levels for F-like ions with $Z = 24$–30 from our MCDHF and MBPT calculations, and the NIST compiled values (Kramida et al. 2016) are also listed. The *LSJ* coupling expansion coefficients for each level are listed as well. Levels are normally labeled as the CSF with the largest expansion coefficient. In cases in which a label has been assigned, the corresponding CSF is removed for the one with the next largest expansion coefficient. We can see that many levels are strongly mixed, for which there are not unique identifications. Here, the parity, J, and energy, rather than level identification, are adopted to match the levels from various sources.

For example, the CSFs with the largest expansion coefficient in levels 33 ($E_{MCDHF} = 6809996\,cm^{-1}$, $E_{MBPT} = 6810824\,cm^{-1}$) and 46 ($E_{MCDHF} = 6917645\,cm^{-1}$, $E_{MBPT} = 6918302\,cm^{-1}$) are $2s^22p^4(^3P)3d\ ^4D_{3/2}$. But this CSF has been used to identify the 33rd level, so the 46th level has to be labeled as the CSF with the second largest coefficient $2s^22p^4(^3P)3d\ ^2D_{3/2}$. The NIST energy for $2s^22p^4(^3P)3d\ ^4D_{3/2}$ ($E_{NIST} = 6919000\,cm^{-1}$) is in much better agreement with our 46th level than the 33rd level, thus we place this NIST energy at the former position rather than the latter one. The cases in which our identifications are different from the NIST ones are listed in Table 2 for reference.

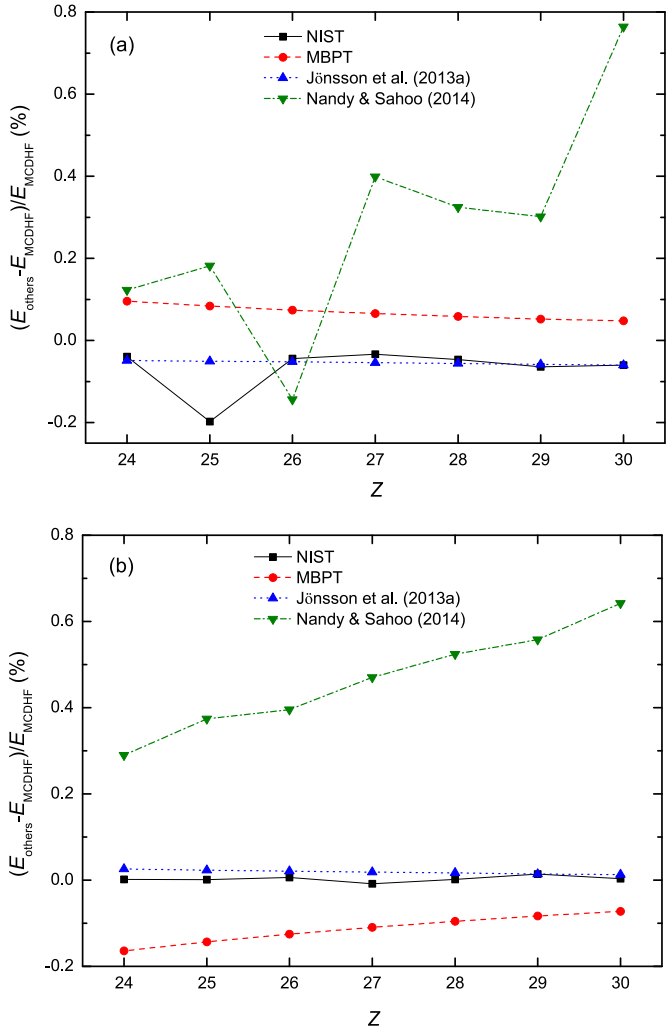

Figure 2. Energy levels from the present MCDHF calculation for the first two excited states $2s^22p^5\ ^2P_{1/2}$ (a) and $2s2p^6\ ^2S_{1/2}$ (b) compared to those from the present MBPT calculation, the NIST compilation (Kramida et al. 2016), Jönsson et al. (2013a), and Nandy & Sahoo (2014).

The present MCDHF and MBPT energy levels show excellent agreement. The absolute differences are within $1500\,cm^{-1}$, except for some doublet levels, but never exceed $4000\,cm^{-1}$. The average differences are generally around $150 \pm 950\,cm^{-1}$. We compared the $n = 3$ and $n = 4$ energy levels from the present MCDHF and MBPT calculations for each ion in Figure 1. The maximum deviations of the two data sets decrease from 0.06% for Cr XVI to 0.03% for Zn XXII ($2s2p^5(^1P)3p\ ^2S_{1/2}$). The average relative differences (with standard deviations) also decrease from $0.003\% \pm 0.016\%$ for Cr XVI to $0.002\% \pm 0.007\%$ for Zn XXII.

In Figure 2, we compare the present MCDHF and MBPT energy levels for the first two excited sates ($2s^22p^5\ ^2P_{1/2}$ and $2s2p^6\ ^2S_{1/2}$), with results from the NIST compilation (Kramida et al. 2016) and other calculations (Jönsson et al. 2013a; Nandy & Sahoo 2014). Our two calculations agrees to within 0.14% for all ions, but more importantly their differences vary smoothly with Z. The MCDHF results agree perfectly with the results by Jönsson et al. (2013a), which is to be expected, since a similar method was employed. The agreement with the NIST values (Kramida et al. 2016) is smoothly within 0.07%, with the exception of $2s^22p^5\ ^2P_{1/2}$ in Mn XVII. The non-smooth

Table 3
Energy Levels (in cm^{-1}) Relative to the Ground State for the Lowest 200 Levels of Fe XVIII

Key	Configuration	Term	E_{MCDHF}	ΔE_{MBPT}	ΔE_{NIST}	$\Delta E_{CHIANTI}$	$\Delta E_{Jonauskas}$	$\Delta E_{Witthoeft}$	ΔE_{Nahar}
1	$2s^22p^5$	$^2P_{3/2}$	0	0	0	0	0	0	0
2	$2s^22p^5$	$^2P_{1/2}$	102624	76	−45	−45	−561	2208	4326
3	$2s2p^6$	$^2S_{1/2}$	1064636	−1335	66	−36	14958	14132	9868
4	$2s^22p^4(^3P)3s$	$^4P_{5/2}$	6220453	1250	1547	1547	−13681	12410	11760
5	$2s^22p^4(^3P)3s$	$^2P_{3/2}$	6247489	977	611	561	−12662	13223	11884
6	$2s^22p^4(^3P)3s$	$^4P_{1/2}$	6299521	1266	10679	1679	−13930	9493	11198
7	$2s^22p^4(^3P)3s$	$^4P_{3/2}$	6317185	1121	715	715	−13656	10670	12661
8	$2s^22p^4(^3P)3s$	$^2P_{1/2}$	6342298	853	302	302	−12677	11415	12579
9	$2s^22p^4(^1D)3s$	$^2D_{5/2}$	6399342	925	658	1858	−11357	14099	17218
10	$2s^22p^4(^1D)3s$	$^2D_{3/2}$	6403198	890	602	602	−11314	14014	17126
11	$2s^22p^4(^3P)3p$	$^4P_{3/2}$	6465739	1055	⋯	⋯	−12743	10882	13854
12	$2s^22p^4(^3P)3p$	$^4P_{5/2}$	6469211	1102	⋯	−6611	−12898	11101	14827
13	$2s^22p^4(^3P)3p$	$^4P_{1/2}$	6496588	959	⋯	⋯	−12489	10419	15016
14	$2s^22p^4(^3P)3p$	$^4D_{7/2}$	6501641	1056	⋯	−7341	−12014	11266	15856
15	$2s^22p^4(^3P)3p$	$^2D_{5/2}$	6502489	895	⋯	−7589	−11766	12037	15436
16	$2s^22p^4(^3P)3p$	$^4D_{1/2}$	6554009	1037	⋯	⋯	−12723	9371	14406
17	$2s^22p^4(^3P)3p$	$^4D_{3/2}$	6555008	810	⋯	⋯	−11266	11623	16282
18	$2s^22p^4(^3P)3p$	$^2S_{1/2}$	6557024	983	⋯	⋯	−12179	10065	15945
19	$2s^22p^4(^1S)3s$	$^2S_{1/2}$	6557571	1112	17529	−6671	−13824	5435	15969
20	$2s^22p^4(^3P)3p$	$^2P_{3/2}$	6571948	885	⋯	⋯	−11746	10123	16274
21	$2s^22p^4(^3P)3p$	$^4D_{5/2}$	6588725	1025	⋯	⋯	−12567	9071	16529
22	$2s^22p^4(^3P)3p$	$^4S_{3/2}$	6591601	928	⋯	⋯	−11972	9894	16670
23	$2s^22p^4(^3P)3p$	$^2P_{1/2}$	6607736	834	⋯	⋯	−11876	10416	17676
24	$2s^22p^4(^3P)3p$	$^2D_{3/2}$	6613421	824	⋯	⋯	−11716	9894	16677
25	$2s^22p^4(^1D)3p$	$^2F_{5/2}$	6646356	769	⋯	⋯	−10013	13903	21009
26	$2s^22p^4(^1D)3p$	$^2F_{7/2}$	6667816	786	⋯	⋯	−10141	12791	21343
27	$2s^22p^4(^1D)3p$	$^2D_{3/2}$	6683061	776	⋯	⋯	−9501	12634	20857
28	$2s^22p^4(^1D)3p$	$^2D_{5/2}$	6695348	783	⋯	⋯	−9644	12474	21618
29	$2s^22p^4(^1D)3p$	$^2P_{3/2}$	6738826	−1324	⋯	574	4140	19864	23045
30	$2s^22p^4(^1D)3p$	$^2P_{1/2}$	6762929	−160	⋯	⋯	−4819	14235	23260
31	$2s^22p^4(^3P)3d$	$^4D_{5/2}$	6804385	835	⋯	⋯	−11826	11785	17424
32	$2s^22p^4(^3P)3d$	$^4D_{7/2}$	6804564	822	⋯	⋯	−11801	13132	18749
33	$2s^22p^4(^3P)3d$	$^4D_{3/2}$	6809996	828	⋯	⋯	−11701	10916	16543
34	$2s^22p^4(^3P)3d$	$^4D_{1/2}$	6819134	785	⋯	⋯	−11469	11731	17150
35	$2s^22p^4(^3P)3d$	$^4F_{9/2}$	6828304	669	⋯	⋯	−10649	14520	20138
36	$2s^22p^4(^1S)3p$	$^2P_{3/2}$	6836243	940	⋯	⋯	−12206	4262	18817
37	$2s^22p^4(^3P)3d$	$^2F_{7/2}$	6839004	396	⋯	⋯	−10126	14283	18360
38	$2s^22p^4(^1S)3p$	$^2P_{1/2}$	6850099	−491	⋯	⋯	−1803	13044	20039
39	$2s^22p^4(^3P)3d$	$^4P_{1/2}$	6855622	686	2578	3078	−10585	13608	18817
40	$2s^22p^4(^3P)3d$	$^4P_{3/2}$	6870934	626	1466	1466	−10062	13379	18967
41	$2s^22p^4(^3P)3d$	$^2F_{5/2}$	6878734	373	1666	266	−9680	14575	19101
42	$2s^22p^4(^3P)3d$	$^2P_{1/2}$	6898206	706	4994	⋯	−11512	10506	18296
43	$2s^22p^4(^3P)3d$	$^4F_{3/2}$	6902518	714	⋯	182	−10737	9710	17254
44	$2s^22p^4(^3P)3d$	$^4F_{5/2}$	6904049	798	−349	−1349	−11294	10731	18455
45	$2s^22p^4(^3P)3d$	$^4F_{7/2}$	6913250	628	⋯	⋯	−11207	12353	20030
46	$2s^22p^4(^3P)3d$	$^2D_{3/2}$	6917645	657	1355	1355	−10963	11211	19114
47	$2s^22p^4(^3P)3d$	$^4P_{5/2}$	6933490	614	⋯	1810	−11180	12526	20092
48	$2s^22p^4(^3P)3d$	$^2P_{3/2}$	6946084	538	1216	916	−10569	13271	21116
49	$2s^22p^4(^3P)3d$	$^2D_{5/2}$	6956007	239	1493	1493	−8782	14023	20433
50	$2s^22p^4(^1D)3d$	$^2G_{7/2}$	6985848	232	⋯	⋯	−8578	13970	22954
51	$2s^22p^4(^1D)3d$	$^2G_{9/2}$	6988331	277	⋯	⋯	−8706	15703	25266
52	$2s^22p^4(^1D)3d$	$^2S_{1/2}$	7013324	233	976	276	−7570	16014	24273
53	$2s^22p^4(^1D)3d$	$^2F_{5/2}$	7013527	441	⋯	73	−8459	15325	24070
54	$2s^22p^4(^1D)3d$	$^2F_{7/2}$	7024270	397	⋯	⋯	−8586	16057	24739
55	$2s^22p^4(^1D)3d$	$^2P_{3/2}$	7037342	234	1058	558	−3892	16626	24254
56	$2s^22p^4(^1D)3d$	$^2D_{5/2}$	7041084	−130	−284	−784	−5098	18909	23289
57	$2s^22p^4(^1D)3d$	$^2D_{3/2}$	7065732	−193	368	4268	−5321	18658	24242

Table 3
(Continued)

Key	Configuration	Term	$E_{\rm MCDHF}$	$\Delta E_{\rm MBPT}$	$\Delta E_{\rm NIST}$	$\Delta E_{\rm CHIANTI}$	$\Delta E_{\rm Jonauskas}$	$\Delta E_{\rm Witthoeft}$	$\Delta E_{\rm Nahar}$
58	$2s^22p^4(^1D)3d$	$^2P_{1/2}$	7073075	33	1125	1025	−2770	18468	26315
59	$2s2p^5(^3P)3s$	$^4P_{5/2}$	7161578	709	24222	⋯	−3685	14795	26381
60	$2s^22p^4(^1S)3d$	$^2D_{5/2}$	7164696	831	1704	−2396	−11088	7307	24009
61	$2s^22p^4(^1S)3d$	$^2D_{3/2}$	7183174	436	1126	−474	−8172	9263	23561
62	$2s2p^5(^3P)3s$	$^4P_{3/2}$	7197130	353	670	284	−2150	15450	27130
63	$2s2p^5(^3P)3s$	$^4P_{1/2}$	7243238	526	−18638	⋯	−3083	14736	28198
64	$2s2p^5(^3P)3s$	$^2P_{3/2}$	7250219	−202	681	305	956	16731	28613
65	$2s2p^5(^3P)3s$	$^2P_{1/2}$	7304198	−226	⋯	365	643	16285	29503
66	$2s2p^5(^3P)3p$	$^4S_{3/2}$	7395295	852	⋯	⋯	−3532	12494	27337
67	$2s2p^5(^3P)3p$	$^4D_{5/2}$	7422724	490	⋯	4476	−1689	14825	28363
68	$2s2p^5(^3P)3p$	$^4D_{7/2}$	7431839	658	⋯	⋯	−2173	13600	28532
69	$2s2p^5(^3P)3p$	$^4D_{3/2}$	7447995	500	16405	1305	−1693	13973	28321
70	$2s2p^5(^3P)3p$	$^2D_{5/2}$	7460866	317	16334	3534	−1316	13962	28486
71	$2s2p^5(^3P)3p$	$^4D_{1/2}$	7474455	403	⋯	⋯	−1372	14470	29405
72	$2s2p^5(^3P)3p$	$^2P_{3/2}$	7487268	365	532	532	−1228	15226	30364
73	$2s2p^5(^3P)3p$	$^2P_{1/2}$	7503954	−308	4146	4146	982	16225	30281
74	$2s2p^5(^3P)3p$	$^4P_{5/2}$	7507510	450	590	590	−1604	14187	30247
75	$2s2p^5(^3P)3p$	$^4P_{3/2}$	7512026	369	17874	⋯	−1484	13828	30000
76	$2s2p^5(^3P)3p$	$^4P_{1/2}$	7517157	453	⋯	⋯	−1752	14273	30718
77	$2s2p^5(^1P)3s$	$^2P_{3/2}$	7520103	−284	⋯	17097	6291	24653	39009
78	$2s2p^5(^1P)3s$	$^2P_{1/2}$	7526471	−409	⋯	10729	7071	24660	39149
79	$2s2p^5(^3P)3p$	$^2D_{3/2}$	7557262	429	9738	⋯	−1898	13286	30964
80	$2s2p^5(^3P)3p$	$^2S_{1/2}$	7577251	−1549	22149	2523	5590	18936	33559
81	$2s2p^5(^3P)3d$	$^4P_{1/2}$	7722864	579	⋯	⋯	−3242	12456	28398
82	$2s2p^5(^3P)3d$	$^4P_{3/2}$	7731650	545	⋯	⋯	−3041	13353	29357
83	$2s2p^5(^3P)3d$	$^4F_{9/2}$	7739704	348	⋯	⋯	−1753	15479	31037
84	$2s2p^5(^3P)3d$	$^4P_{5/2}$	7746896	455	⋯	⋯	−2504	14173	30177
85	$2s2p^5(^3P)3d$	$^4F_{7/2}$	7750799	272	⋯	⋯	−1437	14276	29917
86	$2s2p^5(^1P)3p$	$^2D_{3/2}$	7762208	−407	1192	⋯	7798	25101	42233
87	$2s2p^5(^3P)3d$	$^4F_{5/2}$	7771208	203	⋯	⋯	−1380	14515	30029
88	$2s2p^5(^3P)3d$	$^2F_{7/2}$	7784767	−39	⋯	⋯	−764	16610	30834
89	$2s2p^5(^1P)3p$	$^2D_{5/2}$	7785252	−406	−1352	16248	7744	24181	42552
90	$2s2p^5(^3P)3d$	$^4F_{3/2}$	7788857	150	⋯	⋯	−904	14065	29971
91	$2s2p^5(^1P)3p$	$^2P_{1/2}$	7794271	−279	−8271	⋯	7748	23782	42027
92	$2s2p^5(^1P)3p$	$^2P_{3/2}$	7804850	−239	−10450	⋯	7777	23456	42268
93	$2s2p^5(^3P)3d$	$^4D_{1/2}$	7817935	52	⋯	⋯	−149	14487	30862
94	$2s2p^5(^1P)3p$	$^2S_{1/2}$	7824952	−3648	⋯	⋯	22560	32145	44761
95	$2s2p^5(^3P)3d$	$^2D_{5/2}$	7828946	−114	⋯	⋯	−923	17044	31626
96	$2s2p^5(^3P)3d$	$^4D_{7/2}$	7830553	31	⋯	⋯	−881	16643	32477
97	$2s2p^5(^3P)3d$	$^4D_{5/2}$	7830898	80	⋯	⋯	−683	15213	31803
98	$2s2p^5(^3P)3d$	$^4D_{3/2}$	7839025	123	⋯	⋯	−923	14863	32136
99	$2s2p^5(^3P)3d$	$^2D_{3/2}$	7843195	−201	⋯	−8925	371	16733	31390
100	$2s2p^5(^3P)3d$	$^2P_{1/2}$	7866302	−861	⋯	−1652	4945	19951	31997
101	$2s2p^5(^3P)3d$	$^2F_{5/2}$	7881249	−60	⋯	⋯	−1000	16309	32896
102	$2s2p^5(^3P)3d$	$^2P_{3/2}$	7924316	−934	⋯	−916	4834	20285	33966
103	$2s2p^5(^1P)3d$	$^2F_{5/2}$	8099131	−980	⋯	⋯	10276	25490	40338
104	$2s2p^5(^1P)3d$	$^2F_{7/2}$	8100003	−954	⋯	⋯	10284	27415	42056
105	$2s2p^5(^1P)3d$	$^2P_{3/2}$	8109297	−1268	⋯	⋯	11284	29698	41727
106	$2s2p^5(^1P)3d$	$^2P_{1/2}$	8117127	−1496	⋯	⋯	12359	29968	41019
107	$2s2p^5(^1P)3d$	$^2D_{5/2}$	8128204	−725	⋯	⋯	8282	26673	41410
108	$2s2p^5(^1P)3d$	$^2D_{3/2}$	8128827	−823	⋯	⋯	8702	25309	39986
109	$2s^22p^4(^3P)4s$	$^4P_{5/2}$	8417656	725	⋯	⋯	−10383	14652	68792
110	$2p^63s$	$^2S_{1/2}$	8418105	−2532	⋯	⋯	27491	41186	74126
111	$2s^22p^4(^3P)4s$	$^2P_{3/2}$	8426924	630	1276	⋯	−10292	14389	68829
112	$2s^22p^4(^3P)4s$	$^4P_{1/2}$	8495236	253	⋯	⋯	−5490	11320	67973
113	$2s^22p^4(^3P)4s$	$^4P_{3/2}$	8508688	661	8512	⋯	−10913	11959	69182

Table 3
(Continued)

Key	Configuration	Term	$E_{\rm MCDHF}$	$\Delta E_{\rm MBPT}$	$\Delta E_{\rm NIST}$	$\Delta E_{\rm CHIANTI}$	$\Delta E_{\rm Jonauskas}$	$\Delta E_{\rm Witthoeft}$	$\Delta E_{\rm Nahar}$
114	$2s^22p^4(^3P)4s$	$^2P_{1/2}$	8516141	540	⋯	⋯	−10214	11687	69191
115	$2s^22p^4(^3P)4p$	$^4P_{3/2}$	8519369	427	⋯	⋯	−9936	14193	68871
116	$2s^22p^4(^3P)4p$	$^4P_{5/2}$	8519501	468	⋯	⋯	−10100	14057	68717
117	$2s^22p^4(^3P)4p$	$^4D_{7/2}$	8530427	645	⋯	⋯	−10084	13192	70169
118	$2s^22p^4(^3P)4p$	$^2D_{5/2}$	8531020	521	⋯	⋯	−10009	13434	69346
119	$2s^22p^4(^3P)4p$	$^2S_{1/2}$	8534332	312	⋯	⋯	−9429	13656	70555
120	$2s^22p^4(^3P)4p$	$^2P_{3/2}$	8558366	−202	⋯	⋯	−8463	14189	70202
121	$2s^22p^4(^1D)4s$	$^2D_{5/2}$	8589712	458	1388	⋯	−8673	15092	73797
122	$2s^22p^4(^1D)4s$	$^2D_{3/2}$	8590974	443	2026	⋯	−8683	15001	73841
123	$2s^22p^4(^3P)4p$	$^4D_{1/2}$	8596694	36	⋯	⋯	−5112	10894	67682
124	$2s^22p^4(^3P)4p$	$^4D_{3/2}$	8606168	234	⋯	⋯	−6647	10335	68731
125	$2s^22p^4(^3P)4p$	$^4P_{1/2}$	8606930	384	⋯	⋯	−10175	11876	70384
126	$2s^22p^4(^3P)4p$	$^4D_{5/2}$	8618780	526	⋯	⋯	−10629	10644	70506
127	$2s^22p^4(^3P)4p$	$^4S_{3/2}$	8622454	99	⋯	⋯	−9419	11568	70530
128	$2s^22p^4(^3P)4p$	$^2D_{3/2}$	8626850	322	⋯	⋯	−8867	11045	69843
129	$2s^22p^4(^3P)4p$	$^2P_{1/2}$	8632048	−178	⋯	⋯	−8836	11735	71427
130	$2s^22p^4(^3P)4d$	$^4D_{7/2}$	8644406	648	⋯	⋯	−9982	14198	62175
131	$2s^22p^4(^3P)4d$	$^4D_{5/2}$	8644690	642	⋯	⋯	−9924	13787	61792
132	$2s^22p^4(^3P)4d$	$^4D_{3/2}$	8647125	658	⋯	⋯	−9853	13430	61639
133	$2s^22p^4(^3P)4d$	$^4P_{1/2}$	8650769	678	⋯	⋯	−9721	13561	62045
134	$2s^22p^4(^3P)4d$	$^4F_{9/2}$	8651454	825	⋯	⋯	−9869	14273	63401
135	$2p^63p$	$^2P_{1/2}$	8651848	−2535	⋯	⋯	27610	40889	56115
136	$2s^22p^4(^3P)4d$	$^2F_{7/2}$	8655791	742	⋯	⋯	−9513	14012	62400
137	$2s^22p^4(^3P)4d$	$^2P_{1/2}$	8664235	565	⋯	⋯	−9315	14406	63075
138	$2s^22p^4(^3P)4d$	$^2D_{3/2}$	8673684	279	2316	3116	−9109	14719	62811
139	$2p^63p$	$^2P_{3/2}$	8675769	−2564	⋯	⋯	28560	39897	58871
140	$2s^22p^4(^3P)4d$	$^2D_{5/2}$	8675882	219	118	918	−8928	14906	62753
141	$2s^22p^4(^1D)4p$	$^2F_{5/2}$	8689859	370	⋯	⋯	−8331	14794	74158
142	$2s^22p^4(^1D)4p$	$^2F_{7/2}$	8698580	353	⋯	⋯	−8391	13892	75138
143	$2s^22p^4(^1D)4p$	$^2P_{3/2}$	8701961	−148	⋯	⋯	−7756	14260	75883
144	$2s^22p^4(^1D)4p$	$^2D_{5/2}$	8707674	576	⋯	⋯	−8405	13573	75580
145	$2s^22p^4(^1D)4p$	$^2D_{3/2}$	8708223	−435	⋯	⋯	−7315	14968	75294
146	$2s^22p^4(^3P)4f$	$^4F_{7/2}$	8713450	792	⋯	⋯	−10926	14583	17778
147	$2s^22p^4(^3P)4f$	$^4F_{9/2}$	8713503	798	⋯	⋯	−10947	14818	18021
148	$2s^22p^4(^3P)4f$	$^4F_{5/2}$	8714321	810	⋯	⋯	−10878	14452	17730
149	$2s^22p^4(^3P)4f$	$^2G_{9/2}$	8715646	689	⋯	⋯	−10925	14957	17930
150	$2s^22p^4(^3P)4f$	$^4G_{11/2}$	8715843	738	⋯	⋯	−11017	15033	35796
151	$2s^22p^4(^3P)4f$	$^2F_{7/2}$	8715898	700	⋯	⋯	−11001	15055	18007
152	$2s^22p^4(^3P)4f$	$^4D_{3/2}$	8716491	849	⋯	⋯	−11360	14364	15230
153	$2s^22p^4(^3P)4f$	$^4D_{5/2}$	8718274	754	⋯	⋯	−10965	14949	18265
154	$2s^22p^4(^3P)4f$	$^4D_{1/2}$	8719110	868	⋯	⋯	−10860	14341	18373
155	$2s^22p^4(^3P)4f$	$^2D_{3/2}$	8720325	797	⋯	⋯	−10359	14934	18431
156	$2s^22p^4(^3P)4d$	$^4F_{3/2}$	8726056	301	1444	⋯	−5114	10465	61061
157	$2s^22p^4(^1D)4p$	$^2P_{1/2}$	8726779	−1298	⋯	⋯	−4908	15803	73989
158	$2s^22p^4(^3P)4d$	$^4F_{5/2}$	8728437	396	−937	⋯	−5933	10911	61763
159	$2s^22p^4(^3P)4d$	$^4D_{1/2}$	8734706	489	⋯	⋯	−10188	11384	62594
160	$2s^22p^4(^3P)4d$	$^4F_{7/2}$	8738876	695	⋯	⋯	−10369	11637	63308
161	$2s^22p^4(^3P)4d$	$^4P_{3/2}$	8742234	527	⋯	⋯	−10089	11451	62978
162	$2s^22p^4(^1S)4s$	$^2S_{1/2}$	8746200	−3222	⋯	⋯	18672	6138	72774
163	$2s^22p^4(^3P)4d$	$^4P_{5/2}$	8746546	743	⋯	⋯	−10262	11442	63649
164	$2s^22p^4(^3P)4d$	$^2F_{5/2}$	8755056	157	1544	1544	−8371	12373	63040
165	$2s^22p^4(^3P)4d$	$^2P_{3/2}$	8758783	105	1117	1017	−8542	12426	63625
166	$2s^22p^4(^3P)4f$	$^4G_{5/2}$	8790618	345	⋯	⋯	−5456	11166	18512
167	$2s^22p^4(^3P)4f$	$^2G_{7/2}$	8791487	345	⋯	⋯	−5478	11483	18334
168	$2s^22p^4(^3P)4f$	$^4F_{3/2}$	8803208	796	⋯	⋯	−11386	11683	19694
169	$2s^22p^4(^3P)4f$	$^4G_{9/2}$	8803888	742	⋯	⋯	−11467	12169	19793

Table 3
(Continued)

Key	Configuration	Term	$E_{\rm MCDHF}$	$\Delta E_{\rm MBPT}$	$\Delta E_{\rm NIST}$	$\Delta E_{\rm CHIANTI}$	$\Delta E_{\rm Jonauskas}$	$\Delta E_{\rm Witthoeft}$	$\Delta E_{\rm Nahar}$
170	$2s^22p^4\,(^3P)4f$	$^4G_{7/2}$	8803915	680	⋯	⋯	−11451	12062	19514
171	$2s^22p^4\,(^3P)4f$	$^2F_{5/2}$	8804662	761	⋯	⋯	−11434	12022	19897
172	$2s^22p^4\,(^3P)4f$	$^2D_{5/2}$	8807560	714	⋯	⋯	−11423	11986	19797
173	$2s^22p^4\,(^3P)4f$	$^4D_{7/2}$	8807872	771	⋯	⋯	−11453	12064	19826
174	$2s^22p^4\,(^1D)4d$	$^2G_{7/2}$	8816235	559	⋯	⋯	−8153	14352	67242
175	$2s^22p^4\,(^1D)4d$	$^2G_{9/2}$	8817606	563	⋯	⋯	−8216	14840	68362
176	$2s^22p^4\,(^1D)4d$	$^2D_{5/2}$	8825756	535	3444	3444	−7935	14615	68355
177	$2s^22p^4\,(^1D)4d$	$^2S_{1/2}$	8826721	190	2479	⋯	−7136	14527	68410
178	$2s^22p^4\,(^1D)4d$	$^2P_{3/2}$	8828677	−39	523	523	−7876	14763	67705
179	$2s^22p^4\,(^1D)4d$	$^2F_{7/2}$	8829753	683	⋯	⋯	−8015	14606	68539
180	$2s^22p^4\,(^1D)4d$	$^2F_{5/2}$	8831794	292	−2594	−2594	−7520	14810	67847
181	$2s^22p^4\,(^1D)4d$	$^2D_{3/2}$	8841152	−76	2748	1148	−7118	15693	68015
182	$2s^22p^4\,(^1D)4d$	$^2P_{1/2}$	8844793	−326	−893	−2493	−7688	15448	67874
183	$2s^22p^4\,(^1S)4p$	$^2P_{1/2}$	8856013	−3348	⋯	⋯	20471	6218	76111
184	$2s^22p^4\,(^1S)4p$	$^2P_{3/2}$	8858407	−3139	⋯	⋯	20328	4854	75297
185	$2s^22p^4\,(^1D)4f$	$^2H_{9/2}$	8880153	486	⋯	⋯	−9414	15117	17349
186	$2s^22p^4\,(^1D)4f$	$^2H_{11/2}$	8880875	484	⋯	⋯	−9438	15364	1022
187	$2s^22p^4\,(^1D)4f$	$^2P_{1/2}$	8881342	664	⋯	⋯	−9448	14798	17224
188	$2s^22p^4\,(^1D)4f$	$^2P_{3/2}$	8881963	671	⋯	⋯	−9319	15024	18238
189	$2s^22p^4\,(^1D)4f$	$^2D_{5/2}$	8885492	709	⋯	⋯	−9236	14983	18166
190	$2s^22p^4\,(^1D)4f$	$^2D_{3/2}$	8885641	656	⋯	⋯	−9318	14949	17973
191	$2s^22p^4\,(^1D)4f$	$^2G_{7/2}$	8887996	608	⋯	⋯	−9396	14924	17538
192	$2s^22p^4\,(^1D)4f$	$^2F_{5/2}$	8888465	618	⋯	⋯	−9344	14946	18046
193	$2s^22p^4\,(^1D)4f$	$^2F_{7/2}$	8888653	651	⋯	⋯	−9290	15104	18077
194	$2s^22p^4\,(^1D)4f$	$^2G_{9/2}$	8888781	606	⋯	⋯	−9415	15217	17840
195	$2p^63d$	$^2D_{3/2}$	8979016	−3660	⋯	10084	33896	40350	70691
196	$2s^22p^4\,(^1S)4d$	$^2D_{5/2}$	8979073	−3605	⋯	⋯	19070	6601	79995
197	$2p^63d$	$^2D_{5/2}$	8984723	−2623	⋯	⋯	29136	41003	61341
198	$2s^22p^4\,(^1S)4d$	$^2D_{3/2}$	8985678	−2704	3522	⋯	14062	5625	68100
199	$2s^22p^4\,(^1S)4f$	$^2F_{5/2}$	9041025	−2715	⋯	⋯	19044	5694	17516
200	$2s^22p^4\,(^1S)4f$	$^2F_{7/2}$	9041604	−2692	⋯	⋯	19097	5921	17815

Note. For brevity, energies other than the present MCDHF values are listed as differences from the latter ones in $\rm cm^{-1}$. $E_{\rm MCDHF}$, $\Delta E_{\rm MBPT}$—the present calculations; $\Delta E_{\rm NIST}$—Kramida et al. (2016); $\Delta E_{\rm CHIANTI}$—Dere et al. (1997); Del Zanna et al. (2015); $\Delta E_{\rm Jonauskas}$—Jonauskas et al. (2004); $\Delta E_{\rm Witthoeft}$—Witthoeft et al. (2006); $\Delta E_{\rm Nahar}$—Nahar (2006). $\Delta E_{\rm x} = \Delta E_{\rm x} - E_{\rm MCDHF}$.

behavior along the sequence for this ion indicates that the NIST value is uncertain. The energy levels from Nandy & Sahoo (2014) have the worst agreement with the present MCDHF results, but more severe is the irregular behavior along the isoelectronic sequence for $2s^22p^5\ ^2P_{1/2}$.

Fe XVIII is the most carefully studied system among the F-like ions. Examples are the theoretical studies performed by Jonauskas et al. (2004), Gu (2005b), Witthoeft et al. (2006), and Nahar (2006). Through the review and assessment of line identifications from laboratory and astrophysical observations, Del Zanna (2006) revised and confirmed some level identifications for Fe XVIII. Some of these results are included in the CHIANTI database (Dere et al. 1997; Del Zanna et al. 2015). In Table 3, we compare the present MCDHF and MBPT energy levels for Fe XVIII with those from these earlier calculations and the CHIANTI database (Dere et al. 1997; Del Zanna et al. 2015), as well as the NIST compilation (Kramida et al. 2016). The MBPT values from Gu (2005b) have an accuracy that is similar to the present MBPT results and are therefore omitted in Table 3. We have to point out that the CHIANTI database identified the levels 138, 140, and 164 as $2s^22p^4\,(^3P)4d\ ^4P_{3/2}$, $^2F_{5/2}$, and $^2D_{5/2}$, respectively, which are different from ours. As mentioned earlier, the present MCDHF and MBPT theoretical energy levels are in excellent agreement, differing from each other by only $150 \pm 990\ \rm cm^{-1}$ on average for Fe XVIII. However, energy levels from Jonauskas et al. (2004), Witthoeft et al. (2006), and Nahar (2006) show average differences of $-4633 \pm 9494\ \rm cm^{-1}$, $14741 \pm 6007\ \rm cm^{-1}$, and $37422 \pm 22005\ \rm cm^{-1}$ from the present MCDHF results, with the largest differences being, respectively, $33896\ \rm cm^{-1}$ (195th level, $2p^63d\ ^2D_{3/2}$), $41186\ \rm cm^{-1}$ (110th level, $2p^63s\ ^2S_{1/2}$), and $79995\ \rm cm^{-1}$ (196th level, $2s^22p^4\,(^1S)4d\ ^2D_{5/2}$).

As shown in Table 3, the majority of the results from the NIST and CHIANTI compilations agree well with the present theoretical results, with some exceptions where the differences from the present calculations are larger than $10{,}000\ \rm cm^{-1}$. Moreover, though both the NIST (Kramida et al. 2016) and CHIANTI (Dere et al. 1997; Del Zanna et al. 2015) values are critically evaluated, there are some inconsistencies. For these cases, the present theoretical results agree well with one of the databases and can therefore resolve these discrepancies. For example, energies for $2s^22p^4\,(^3P)3s\ ^4P_{1/2}$ from the present MCDHF and MBPT calculations agree

Table 4
Energy Levels (in cm^{-1}) Relative to the Ground State for Levels in Which the NIST Values Kramida et al. (2016) Differ from the Present MCDHF Values by More than 4000 cm^{-1} (0.05%)

Z	Key	Configuration	Term	E_{MCDHF}	ΔE_{MBPT}	ΔE_{NIST}	Z	Key	Configuration	Term	E_{MCDHF}	ΔE_{MBPT}	ΔE_{NIST}
27	19	$2s^22p^4(^1S)3s$	$^2S_{1/2}$	7227255	1081	16645	28	140	$2s^22p^4(^3P)4d$	$^2D_{5/2}$	10468378	165	−6378
27	33	$2s^22p^4(^3P)3d$	$^4D_{3/2}$	7477646	799	142554	28	157	$2s^22p^4(^3P)4d$	$^4F_{5/2}$	10537333	130	−7333
27	47	$2s^22p^4(^3P)3d$	$^4P_{5/2}$	7621037	603	−71637	28	165	$2s^22p^4(^3P)4d$	$^2P_{3/2}$	10586571	151	−5571
27	56	$2s^22p^4(^1D)3d$	$^2D_{5/2}$	7731984	−129	−5184	28	180	$2s^22p^4(^1D)4d$	$^2P_{3/2}$	10660222	−44	−5222
27	62	$2s^22p^4(^1S)3d$	$^2D_{3/2}$	7892516	376	24884	28	182	$2s^22p^4(^1D)4d$	$^2F_{5/2}$	10664116	277	12884
27	67	$2s2p^5(^3P)3p$	$^4D_{5/2}$	8128707	513	14293	28	184	$2s^22p^4(^1D)4d$	$^2P_{1/2}$	10680974	−372	−6974
27	69	$2s2p^5(^3P)3p$	$^4D_{3/2}$	8158501	527	12499	29	14	$2s^22p^4(^3P)3p$	$^2D_{5/2}$	8541967	834	24033
27	70	$2s2p^5(^3P)3p$	$^2D_{5/2}$	8172198	352	16802	29	18	$2s^22p^4(^3P)3p$	$^4P_{1/2}$	8640869	958	23131
27	72	$2s2p^5(^3P)3p$	$^2P_{3/2}$	8202709	395	15291	29	20	$2s^22p^4(^1S)3s$	$^2S_{1/2}$	8672489	1017	17511
27	73	$2s2p^5(^3P)3p$	$^2P_{1/2}$	8218999	−294	8001	29	22	$2s^22p^4(^3P)3p$	$^4D_{5/2}$	8692331	979	−22331
27	75	$2s2p^5(^3P)3p$	$^2D_{3/2}$	8232447	399	19553	29	25	$2s^22p^4(^1D)3p$	$^2F_{5/2}$	8742018	704	4982
27	79	$2s2p^5(^3P)3p$	$^4P_{3/2}$	8287351	475	15649	29	36	$2s^22p^4(^3P)3d$	$^2F_{7/2}$	8936506	338	8494
27	80	$2s2p^5(^3P)3p$	$^2S_{1/2}$	8302784	−1341	20216	29	43	$2s^22p^4(^3P)3d$	$^4F_{5/2}$	9036992	726	−29992
27	91	$2s2p^5(^1P)3p$	$^2P_{1/2}$	8526446	−236	−5446	29	44	$2s^22p^4(^3P)3d$	$^4D_{1/2}$	9048382	708	29618
27	92	$2s2p^5(^1P)3p$	$^2P_{3/2}$	8539038	−192	−8038	29	45	$2s^22p^4(^3P)3d$	$^4F_{7/2}$	9071401	625	−5401
27	111	$2s^22p^4(^3P)4s$	$^2P_{3/2}$	9285675	615	−5675	29	46	$2s^22p^4(^3P)3d$	$^2D_{3/2}$	9072726	657	6274
27	115	$2s^22p^4(^3P)4s$	$^4P_{3/2}$	9385062	646	8938	29	50	$2s^22p^4(^1D)3d$	$^2G_{7/2}$	9149844	205	4156
27	123	$2s^22p^4(^1D)4s$	$^2D_{5/2}$	9468381	435	−6381	29	62	$2s^22p^4(^1S)3d$	$^2D_{3/2}$	9419131	278	8869
27	124	$2s^22p^4(^1D)4s$	$^2D_{3/2}$	9469918	418	−5918	29	67	$2s2p^5(^3P)3p$	$^4D_{5/2}$	9638903	569	19097
27	140	$2s^22p^4(^3P)4d$	$^2D_{5/2}$	9551443	188	−6443	29	69	$2s2p^5(^3P)3p$	$^2P_{3/2}$	9679756	598	14244
27	178	$2s^22p^4(^1D)4d$	$^2P_{3/2}$	9722454	−50	−4454	29	70	$2s2p^5(^3P)3p$	$^4P_{5/2}$	9695337	433	21663
27	180	$2s^22p^4(^1D)4d$	$^2F_{5/2}$	9725977	275	6023	29	72	$2s2p^5(^3P)3p$	$^4D_{3/2}$	9734565	458	12435
27	181	$2s^22p^4(^1D)4d$	$^2D_{3/2}$	9736521	−103	−4521	29	73	$2s2p^5(^3P)3p$	$^2P_{1/2}$	9748866	−230	22134
27	182	$2s^22p^4(^1D)4d$	$^2P_{1/2}$	9740861	−353	−8861	29	75	$2s2p^5(^3P)3p$	$^2D_{5/2}$	9771060	544	29940
27	198	$2s^22p^4(^1S)4d$	$^2D_{3/2}$	9897499	−3040	22501	29	76	$2s2p^5(^3P)3p$	$^2D_{3/2}$	9776300	472	15700
28	14	$2s^22p^4(^3P)3p$	$^2D_{5/2}$	7831603	842	22097	29	79	$2s2p^5(^3P)3p$	$^4P_{3/2}$	9856325	577	15675
28	18	$2s^22p^4(^3P)3p$	$^4P_{1/2}$	7912967	960	17833	29	80	$2s2p^5(^3P)3p$	$^2S_{1/2}$	9859383	−987	34617
28	20	$2s^22p^4(^1S)3s$	$^2S_{1/2}$	7932063	1044	16937	30	4	$2s^22p^4(3P^)3s$	$^4P_{5/2}$	8924021	1166	4979
28	22	$2s^22p^4(^3P)3p$	$^4D_{5/2}$	7957767	989	−20967	30	5	$2s^22p^4(3P^)3s$	$^2P_{3/2}$	8956413	896	8587
28	25	$2s^22p^4(^1D)3p$	$^2F_{5/2}$	8010940	718	4760	30	6	$2s^22p^4(3P^)3s$	$^4P_{1/2}$	9044217	1121	6783
28	36	$2s^22p^4(^3P)3d$	$^2F_{7/2}$	8206845	351	7355	30	21	$2s^22p^4(^1S)3s$	$^2S_{1/2}$	9449026	994	11974
28	43	$2s^22p^4(^3P)3d$	$^4F_{5/2}$	8294866	748	−26866	30	44	$2s^22p^4(^3P)3d$	$^4D_{1/2}$	9832441	709	11559
28	44	$2s^22p^4(^3P)3d$	$^2P_{1/2}$	8298153	703	5847	30	53	$2s^22p^4(^1D)3d$	$^2S_{1/2}$	9971458	251	4542
28	45	$2s^22p^4(^3P)3d$	$^4F_{7/2}$	8318476	621	−5976	30	67	$2s2p^5(^3P)3p$	$^4D_{5/2}$	10443507	599	14493
28	46	$2s^22p^4(^3P)3d$	$^2D_{3/2}$	8320897	654	8103	30	69	$2s2p^5(^3P)3p$	$^2P_{3/2}$	10491064	627	14936
28	50	$2s^22p^4(^1D)3d$	$^2G_{7/2}$	8395187	208	4313	30	70	$2s2p^5(^3P)3p$	$^4P_{5/2}$	10507679	473	25321
28	55	$2s^22p^4(^1D)3d$	$^2P_{3/2}$	8449900	232	−4900	30	72	$2s2p^5(^3P)3p$	$^4D_{3/2}$	10551240	492	10760
28	69	$2s2p^5(^3P)3p$	$^4D_{3/2}$	8902330	558	5670	30	73	$2s2p^5(^3P)3p$	$^2P_{1/2}$	10564072	−193	28928
28	70	$2s2p^5(^3P)3p$	$^4P_{5/2}$	8916934	388	−8934	30	76	$2s2p^5(^3P)3p$	$^2D_{3/2}$	10600176	498	11824
28	72	$2s2p^5(^3P)3p$	$^2P_{3/2}$	8951760	425	10240	30	79	$2s2p^5(^3P)3p$	$^2S_{1/2}$	10691192	−827	23808
28	73	$2s2p^5(^3P)3p$	$^2P_{1/2}$	8967239	−271	10761	30	91	$2s2p^5(^1P)3p$	$^2P_{1/2}$	10935353	−121	−4353
28	76	$2s2p^5(^3P)3p$	$^2D_{3/2}$	8987129	431	20871	30	92	$2s2p^5(^1P)3p$	$^2P_{3/2}$	10955142	−32	−4142
28	80	$2s2p^5(^3P)3p$	$^2S_{1/2}$	9063374	−1160	28626	30	120	$2s^22p^4(^3P)4s$	$^4P_{3/2}$	12277104	640	183896
28	86	$2s2p^5(^1P)3p$	$^2D_{3/2}$	9254160	−293	−4160	30	139	$2s^22p^4(^3P)4d$	$^2D_{3/2}$	12422681	202	4319
28	89	$2s2p^5(^1P)3p$	$^2D_{5/2}$	9287674	−291	−4674	30	154	$2s^22p^4(^3P)4d$	$^4F_{3/2}$	12503387	−135	7613
28	91	$2s2p^5(^1P)3p$	$^2P_{1/2}$	9293634	−197	−5634	30	180	$2s^22p^4(^1D)4d$	$^2P_{3/2}$	12668710	−27	5290
28	92	$2s2p^5(^1P)3p$	$^2P_{3/2}$	9308441	−144	−5441	30	184	$2s^22p^4(^1D)4d$	$^2P_{1/2}$	12694470	−394	−5470
28	119	$2s^22p^4(^3P)4s$	$^4P_{3/2}$	10305103	640	11897	30	198	$2s^22p^4(^1S)4d$	$^2D_{3/2}$	12916429	−3003	24571

Note. Energies other than the present MCDHF values are listed as differences from the latter ones in cm^{-1}. E_{MCDHF}, ΔE_{MBPT}—the present calculations; ΔE_{NIST}—Kramida et al. (2016). $\Delta E_x = E_x - E_{MCDHF}$.

with the CHIANTI values, as well as the observations from Gordon et al. (1980) by within 1700 cm^{-1}, but differ from the NIST values by more than 10,000 cm^{-1}. On the other hand, the CHIANTI energy for $2s2p^5(^1P)3p\ ^2D_{5/2}$, which was derived from a blended line, differs from the present calculations by over 15,000 cm^{-1}, while the value from the NIST compilation agrees with our calculations by within 1400 cm^{-1}.

Table 5

Wavelengths λ (in Å), Transition Rates A (in s^{-1}), Oscillator Strengths gf (Dimensionless), and Line Strengths S (in au) for Transitions among the Lowest 200 Levels in F-like Ions with $Z = 24$–30

Z	j	i	Type	λ_{MCDHF}	λ_{MBPT}	A_{MCDHF}	gf_{MCDHF}	S_{MCDHF}	A_{MBPT}	gf_{MBPT}	S_{MBPT}
24	2	1	M1	1.4100E+03	1.4087E+03	6.395E+03	3.812E−06	1.329E+00	6.369E+03	3.790E−06	1.320E+00
24	3	1	E1	1.0664E+02	1.0681E+02	6.336E+10	2.160E−01	7.584E−02	6.247E+10	2.137E−01	7.513E−02
24	3	2	E1	1.1536E+02	1.1557E+02	2.467E+10	9.843E−02	3.738E−02	2.431E+10	9.735E−02	3.704E−02
24	4	1	E1	1.9813E+01	1.9808E+01	3.985E+10	1.407E−02	9.178E−04	3.973E+10	1.402E−02	9.142E−04
24	5	1	E1	1.9720E+01	1.9716E+01	9.424E+11	2.198E−01	1.427E−02	9.420E+11	2.196E−01	1.425E−02
24	5	2	E1	2.0000E+01	1.9996E+01	3.356E+10	8.051E−03	5.301E−04	3.370E+10	8.079E−03	5.319E−04
24	6	1	E1	1.9585E+01	1.9580E+01	3.660E+10	4.210E−03	2.714E−04	3.610E+10	4.149E−03	2.675E−04
24	6	2	E1	1.9861E+01	1.9856E+01	1.507E+10	1.783E−03	1.166E−04	1.478E+10	1.748E−03	1.142E−04
24	7	1	E1	1.9547E+01	1.9542E+01	6.806E+11	1.559E−01	1.004E−02	6.658E+11	1.525E−01	9.810E−03
24	7	2	E1	1.9822E+01	1.9817E+01	6.045E+10	1.424E−02	9.294E−04	5.964E+10	1.405E−02	9.163E−04

Note. Only transitions with a branching ratio of over 1% are presented. The indices used to represent the lower (i) and upper (j) levels of a transition refer to the ordering in Table 1.

(This table is available in its entirety in machine-readable form.)

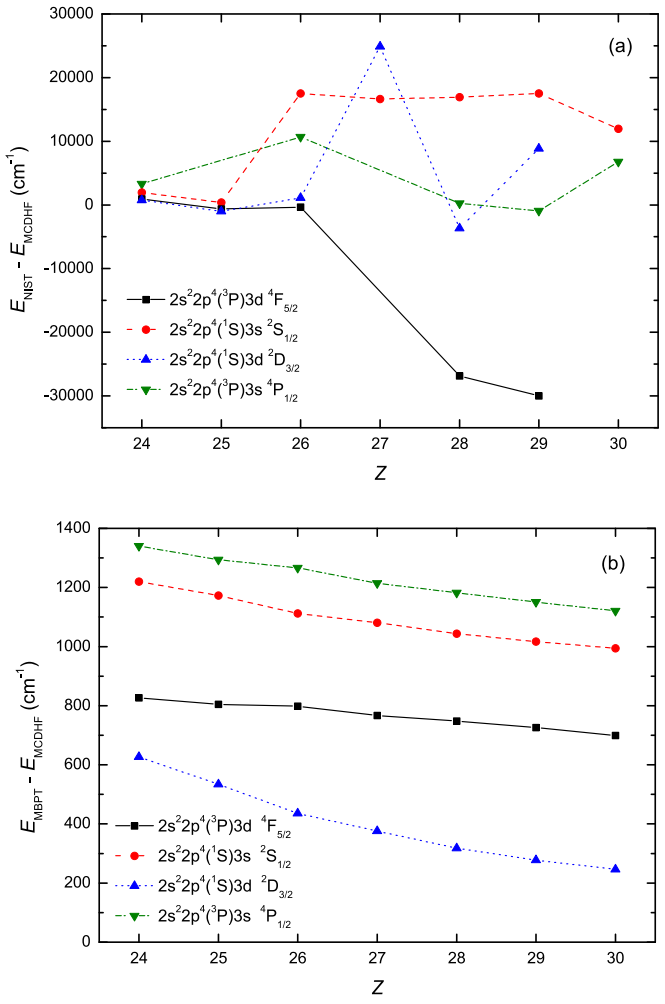

Figure 3. Differences for NIST (Kramida et al. 2016) (a) and the present MBPT (b) energy levels from the present MCDHF values as a function of Z for some levels.

Of all the entire 307 NIST complied energy levels for F-like ions with $Z = 24$–30, which have been included in Table 1, values for $Z = 24$, 25 agree well with the present calculations. However, about 100 values for other ions differ from our MCDHF results by over 0.05% (4000 cm^{-1}). These levels for $Z = 27$–30 are listed in Table 4 to highlight cases that need revised NIST values.

In Figure 3(a), we show the differences between the NIST energy levels and the present MCDHF values as a function of Z for some levels. As can be seen, there are some obvious anomalies along the sequence and some of the NIST compilations deviate from the present MCDHF values by more than 10,000 cm^{-1}. At the same time, the differences between the present MCDHF and MBPT values vary smoothly within 1400 cm^{-1} along the sequence, as shown in Figure 3(b). Line blending or large experimental errors of the spectral observations compiled by NIST are most likely responsible for the large differences with the present theoretical results.

3.2. Wavelengths

In Table 5 we present wavelengths from our two sets of calculations for strong transitions with a branching fraction of over 1%. The overall agreement between the present two sets of wavelengths is within 0.1%.

In Table 6, we compare our computed wavelengths for Fe XVIII with the observed values compiled by NIST (Kramida et al. 2016) and CHIANTI (Dere et al. 1997; Del Zanna et al. 2015) for the lines that are predicted to be the brightest, at both low densities (10^{12} cm^{-3}, astrophysical plasmas) and high densities (10^{19} cm^{-3}, laser plasmas) (Del Zanna 2006). The present MCDHF and MBPT wavelengths listed generally agree to within 0.02%, with two exceptions being the 3–1 and 3–2 transitions, which have differences larger than 0.1%. Our values also mostly agree with observed values compiled in NIST and CHIANTI to within 0.05%, which shows a significant improvement over the results from Jonauskas et al. (2004) and Nahar (2006).

A comparison of the wavelengths for the brightest $\Delta n \neq 0$ transitions in Fe XVIII (Del Zanna 2006) is given in Figure 4. It is clear that the absolute differences between the present MCDHF and MBPT wavelengths for these transitions are mostly within 3 mÅ and no more than 5 mÅ. The present MCDHF wavelengths for $\Delta n \neq 0$ transitions mostly agree to within the error bars of the CHIANTI values except for six transitions, where the differences are larger than 10 mÅ (19, 89 − 1; 19 − 2; 77, 78, 99 − 3). These six observed lines are all blended, which might be the reason for the disagreement. Five NIST wavelengths (43, 69, 70 − 1; 19, 80 − 2) differ from the present MCDHF

Table 6
Wavelength λ (in Å) and Transition Rates A (in s^{-1}) for the Brightest Lines in Fe XVIII (Del Zanna 2006)

j	i	λ_{MCDHF}	λ_{MBPT}	$\lambda_{CHIANTI}$	λ_{NIST}	A_{MCDHF}	A_{MBPT}	$A_{CHIANTI}$	$A_{Jonauskas}$	A_{Nahar}
2	1	974.42	973.71	974.8602	974.86	1.94E+04	1.93E+04	1.94E+04	1.91E+04	1.94E+04
3	1	93.929	94.047	93.9322	93.926	7.76E+10	7.67E+10	8.08E+10	8.31E+10	7.75E+10
4	1	16.076	16.073	16.0720	16.072	8.30E+10	8.28E+10	8.34E+10	8.31E+10	8.44E+10
5	1	16.006	16.004	16.0050	16.005	1.62E+12	1.61E+12	1.61E+12	1.65E+12	1.66E+12
6	1	15.874	15.871	15.8700	⋯	1.72E+11	1.71E+11	1.76E+11	1.70E+11	1.88E+11
7	1	15.830	15.827	15.8281	15.828	7.94E+11	7.81E+11	7.97E+11	8.60E+11	7.65E+11
8	1	15.767	15.765	15.7664	15.766	1.17E+12	1.16E+12	1.16E+12	1.23E+12	1.19E+12
9	1	15.627	15.624	15.6221	15.625	9.74E+11	9.68E+11	9.66E+11	1.02E+12	9.68E+11
19	1	15.250	15.247	15.2651	⋯	2.18E+11	2.16E+11	2.14E+11	2.29E+11	2.09E+11
39	1	14.587	14.585	14.5800	14.581	2.72E+12	2.72E+12	2.75E+12	2.64E+12	2.78E+12
40	1	14.554	14.553	14.5510	14.551	3.52E+12	3.52E+12	3.35E+12	3.27E+12	3.44E+12
41	1	14.538	14.537	14.5370	14.534	4.64E+12	4.65E+12	4.32E+12	4.31E+12	4.56E+12
43	1	14.487	14.486	14.4871	14.453	6.81E+11	6.71E+11	7.05E+11	6.76E+11	7.35E+11
44	1	14.484	14.483	14.4871	⋯	4.28E+08	2.78E+08	5.95E+09	⋯	5.22E+07
46	1	14.456	14.454	14.4530	14.453	8.47E+11	8.26E+11	1.03E+12	9.27E+11	1.02E+12
47	1	14.423	14.421	14.4190	⋯	4.06E+11	3.84E+11	3.32E+11	4.00E+11	3.94E+11
48	1	14.397	14.395	14.3947	⋯	2.51E+11	2.52E+11	2.80E+11	2.29E+11	3.25E+11
49	1	14.376	14.376	14.3730	14.373	7.04E+12	7.03E+12	7.13E+12	6.91E+12	7.66E+12
52	1	14.259	14.258	14.2580	14.256	1.42E+13	1.41E+13	1.13E+12	1.47E+13	1.49E+13
53	1	14.258	14.257	14.2580	⋯	1.42E+12	1.42E+12	1.50E+13	1.36E+12	1.26E+12
55	1	14.210	14.209	14.2088	⋯	1.83E+13	1.80E+13	1.94E+13	1.93E+13	1.83E+13
56	1	14.202	14.203	14.2040	14.203	1.81E+13	1.76E+13	2.05E+13	1.99E+13	1.84E+13
57	1	14.153	14.153	14.1443	14.152	3.44E+12	3.33E+12	4.06E+12	3.94E+12	3.55E+12
60	1	13.957	13.956	13.9620	13.954	1.04E+12	1.04E+12	1.18E+12	1.15E+12	9.94E+11
67	1	13.472	13.471	13.4640	⋯	7.22E+11	7.24E+11	6.43E+11	7.23E+11	7.27E+11
69	1	13.426	13.426	13.4241	13.397	1.18E+12	1.18E+12	1.21E+12	1.18E+12	1.23E+12
70	1	13.403	13.403	13.3969	13.374	1.63E+12	1.61E+12	1.57E+12	1.67E+12	1.67E+12
72	1	13.356	13.355	13.3551	13.355	2.27E+12	2.24E+12	2.22E+12	2.39E+12	2.33E+12
73	1	13.326	13.327	13.3190	13.319	3.49E+12	3.48E+12	3.34E+12	3.48E+12	3.55E+12
74	1	13.320	13.319	13.3190	13.319	1.16E+12	1.14E+12	1.11E+12	1.18E+12	1.16E+12
89	1	12.845	12.845	12.8181	12.847	8.65E+11	8.54E+11	8.61E+11	9.16E+11	8.66E+11
138	1	11.529	11.529	11.5250	11.526	3.49E+12	3.34E+12	3.94E+12	3.73E+12	3.54E+12
140	1	11.526	11.526	11.5250	11.526	4.16E+12	4.00E+12	4.51E+12	4.38E+12	4.17E+12
164	1	11.422	11.422	11.4200	11.420	4.28E+12	3.99E+12	5.09E+12	4.60E+12	4.32E+12
177	1	11.329	11.329	⋯	11.326	5.07E+12	4.99E+12	5.53E+12	5.36E+12	5.39E+12
178	1	11.327	11.327	11.3261	11.326	4.34E+12	4.18E+12	4.99E+12	4.78E+12	4.40E+12
180	1	11.323	11.322	11.3261	11.326	2.88E+12	2.59E+12	2.95E+12	3.15E+12	2.87E+12
3	2	103.95	104.10	103.948	103.939	2.82E+10	2.78E+10	2.95E+10	3.04E+10	2.81E+10
5	2	16.274	16.271	16.2722	16.272	4.13E+10	4.13E+10	4.29E+10	4.34E+10	4.17E+10
7	2	16.091	16.089	16.0893	16.087	6.64E+10	6.58E+10	6.92E+10	7.10E+10	6.45E+10
8	2	16.026	16.024	16.0256	16.026	1.35E+12	1.34E+12	1.34E+12	1.40E+12	1.34E+12
10	2	15.872	15.870	15.8700	15.870	1.19E+12	1.19E+12	1.20E+12	1.24E+12	1.19E+12
19	2	15.492	15.490	15.5079	15.450	8.50E+11	8.40E+11	8.31E+11	8.91E+11	8.56E+11
40	2	14.775	14.774	14.7715	14.772	4.53E+11	4.57E+11	4.21E+11	4.40E+11	4.64E+11
46	2	14.673	14.672	14.6705	⋯	7.13E+11	7.00E+11	7.69E+11	7.65E+11	7.55E+11
48	2	14.612	14.612	14.6105	14.610	1.11E+12	1.12E+12	1.09E+12	1.05E+12	1.25E+12
52	2	14.470	14.470	14.4697	14.469	2.57E+12	2.57E+12	1.69E+03	2.81E+12	2.60E+12
55	2	14.420	14.420	14.4190	14.418	2.64E+12	2.60E+12	2.96E+12	2.84E+12	2.61E+12
57	2	14.361	14.362	14.3525	14.361	1.36E+13	1.35E+13	1.33E+13	1.33E+13	1.33E+13
58	2	14.346	14.346	14.3441	14.344	2.05E+13	2.02E+13	2.21E+13	2.13E+13	2.12E+13
61	2	14.123	14.122	14.1241	14.121	1.29E+13	1.26E+13	1.48E+13	1.44E+13	1.33E+13
80	2	13.379	13.382	13.3740	13.355	3.30E+12	3.28E+12	3.25E+12	3.32E+12	3.34E+12
165	2	11.552	11.552	11.5511	11.551	2.57E+12	2.44E+12	2.92E+12	2.86E+12	2.68E+12
178	2	11.460	11.460	11.4592	⋯	1.10E+12	1.05E+12	1.21E+12	1.22E+12	1.06E+12
181	2	11.444	11.444	11.4420	11.440	4.62E+12	4.38E+12	5.30E+12	5.04E+12	4.55E+12
182	2	11.439	11.439	11.4420	11.440	7.54E+12	7.29E+12	8.83E+12	8.09E+12	7.79E+12
198	2	11.257	11.261	11.2530	11.253	2.86E+12	2.46E+12	3.72E+12	2.09E+12	9.37E+11
29	3	17.624	17.624	17.6218	⋯	2.87E+10	2.74E+10	3.78E+10	3.68E+10	2.57E+10
62	3	16.307	16.302	16.3058	⋯	4.89E+11	4.97E+11	4.91E+11	4.54E+11	5.10E+11
64	3	16.167	16.164	16.1658	⋯	7.33E+11	7.12E+11	7.57E+11	8.60E+11	7.64E+11
65	3	16.027	16.024	16.0258	⋯	1.37E+12	1.34E+12	1.39E+12	1.51E+12	1.42E+12
77	3	15.491	15.488	15.4498	⋯	8.54E+11	8.42E+11	8.78E+11	8.83E+11	8.51E+11
78	3	15.475	15.473	15.4498	⋯	3.40E+11	3.35E+11	3.78E+11	3.51E+11	3.26E+11
99	3	14.752	14.750	14.7718	⋯	2.84E+12	2.86E+12	2.33E+12	2.51E+12	2.83E+12

Table 6
(Continued)

j	i	$\lambda_{\rm MCDHF}$	$\lambda_{\rm MBPT}$	$\lambda_{\rm CHIANTI}$	$\lambda_{\rm NIST}$	$A_{\rm MCDHF}$	$A_{\rm MBPT}$	$A_{\rm CHIANTI}$	$A_{\rm Jonauskas}$	$A_{\rm Nahar}$
100	3	14.702	14.701	14.7058	⋯	1.20E+13	1.17E+13	1.32E+13	1.28E+13	1.25E+13
102	3	14.578	14.577	14.5798	⋯	1.39E+13	1.37E+13	1.49E+13	1.46E+13	1.46E+13
105	3	14.195	14.195	⋯	⋯	1.32E+13	1.30E+13	1.40E+13	1.37E+13	1.36E+13
106	3	14.179	14.180	⋯	⋯	1.82E+13	1.78E+13	2.00E+13	1.94E+13	1.88E+13
12	4	402.00	402.24	415.6284	⋯	3.44E+09	3.40E+09	3.19E+09	⋯	5.26E+09
14	4	355.63	355.88	367.2427	⋯	5.45E+09	5.38E+09	5.09E+09	⋯	8.04E+09
15	5	392.16	392.28	405.1051	⋯	3.94E+09	3.90E+09	3.70E+09	⋯	2.70E+09

Note. MCDHF, MBPT—the present calculations; CHIANTI—Dere et al. (1997); Del Zanna et al. (2015); NIST—Kramida et al. (2016); Jonauskas—Jonauskas et al. (2004); Nahar—Nahar (2006).

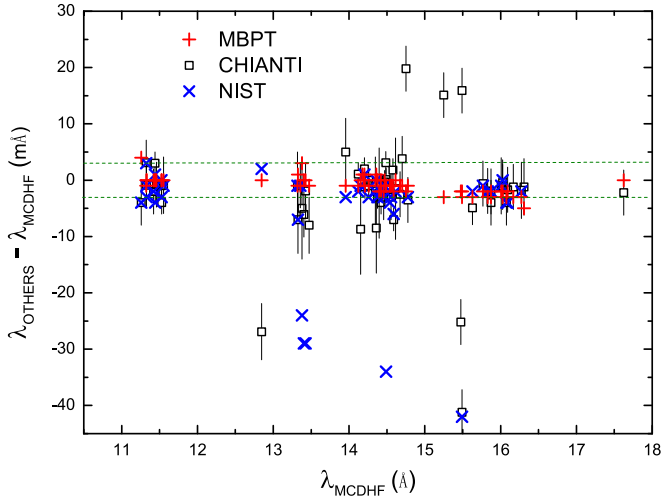

Figure 4. Differences between wavelengths for the present MBPT, NIST (Kramida et al. 2016), and CHIANTI (Dere et al. 1997; Del Zanna et al. 2015) results and the present MCDHF results for the brightest $\Delta n \neq 0$ lines of Fe XVIII (Del Zanna 2006). The horizontal lines indicate differences of ±3 mÅ.

values by more than 20 mÅ, but fortunately, the present MCDHF results agree with the CHIANTI compilations to within 6 mÅ for four of them (the exception is 19 − 2). However, it should also be pointed out that the differences between CHIANTI wavelengths and the present MCDHF values for 12, 14 − 4 and 15–5 are larger than 3%, which implies that these observations either have large errors or the identification is wrong.

3.3. Transition Rates

In Table 5, we also give our two sets of transition rates, along with oscillator strengths and line strengths.

For transition rates from the first two excited energy levels ($2s^22p^5\ ^2P_{1/2}$ and $2s2p^6\ ^2S_{1/2}$), the present MCDHF and MBPT results show excellent agreement with calculations performed by Jönsson et al. (2013a) and Nandy & Sahoo (2014); the differences are all within 1.5%.

The overall agreement between the present MCDHF and MBPT transition rates is within 5%. The transitions with larger differences mostly occur for the ones with large cancellation effects. The examples of $2p^63s\ ^2S_{1/2} - 2s^22p^5\ ^2P_{3/2}$ and $2s^22p^4\,(^3P)3d\ ^4F_{5/2} - 2s^22p^5\ ^2P_{3/2}$ are shown in Figure 5. Figure 5(a) illustrates how the crossing of the $2s^22p^4\,(^3P)4s\ ^2P_{1/2}$ and $2p^63s\ ^2S_{1/2}$ levels at $Z = 25$, which results in strong level mixing, leads to an abrupt change in

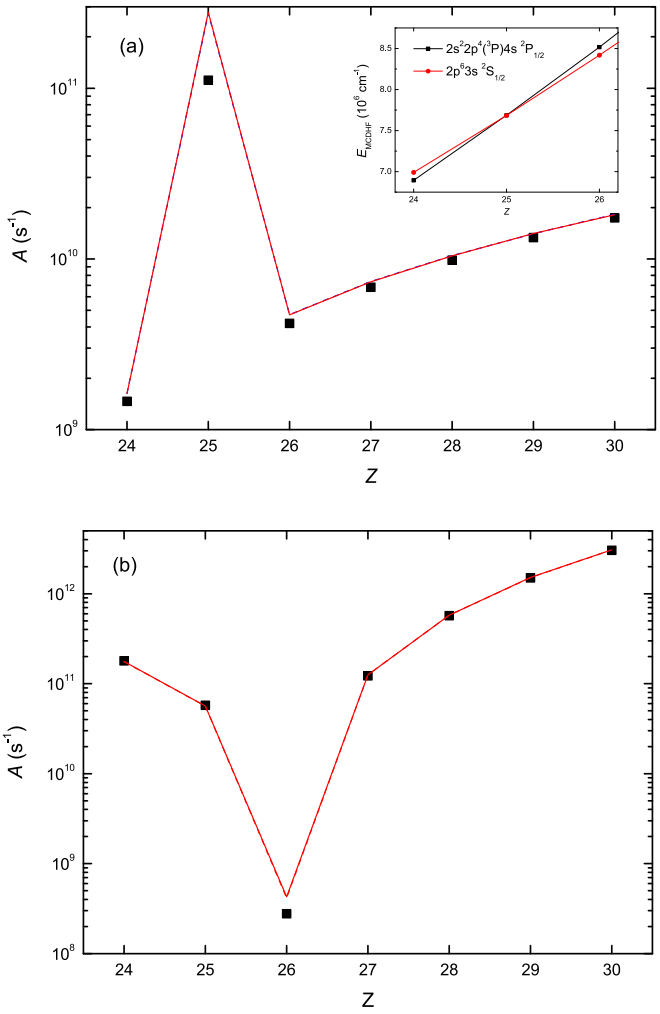

Figure 5. The present MCDHF length (solid line) and velocity (dashed line) form transition rates, as well as those from the present MBPT calculation (square) for $2p^63s\ ^2S_{1/2} - 2s^22p^5\ ^2P_{3/2}$ (a) and $2s^22p^4\,(^3P)3d\ ^4F_{5/2} - 2s^22p^5\ ^2P_{3/2}$ (b) as a function of Z. The inset in (a) shows the energies of $2s^22p^4\,(^3P)4s\ ^2P_{1/2}$ and $2p^63s\ ^2S_{1/2}$ along the sequence.

transition rates. In these cases even a slight difference in the calculations will lead to a relatively large difference in the computed S and A values. Expressed in a different way, the drastic cancellation for $2s^22p^4\,(^3P)3d\ ^4F_{5/2} - 2s^22p^5\ ^2P_{3/2}$ at $Z = 26$ leads to the transition rates being very sensitive to several small perturbations such as core polarization and configuration interaction. Transition rates for such cases are

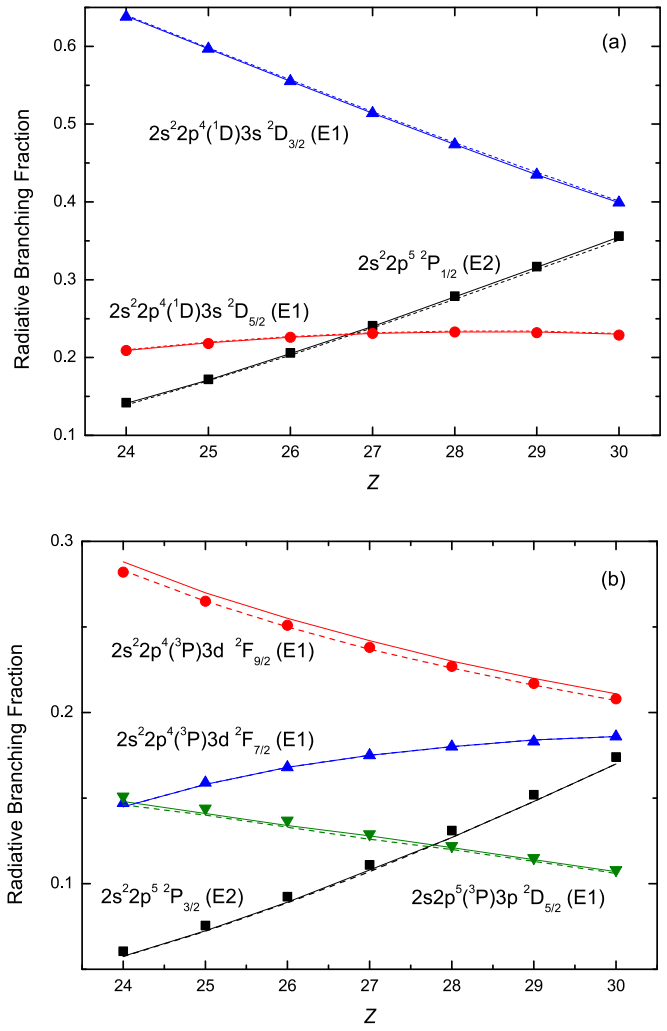

Figure 6. Radiative branching fractions of $2s^22p^4(^1D)3p\ ^2F_{5/2}$ (a) and $2s2p^5(^3P)3d\ ^2F_{7/2}$ (b) from the present MCDHF length (solid line) and velocity (dashed line) form calculation, as well as the present MBPT calculation (scattered).

hard to calculate accurately and will required detailed and focused study. It is also shown in this figure that the present MCDHF transition rates in length L and velocity V forms mostly agree to within 2%.

In Table 6, we compare the present MCDHF and MBPT transition rates for the brightest lines in Fe XVIII with earlier calculations and CHIANTI. The present two sets of transition rates show good agreement (for 66 out of the 72 cases to within 5%), the only exception being the 26–1 transition, which differs by over 10%, and which was discussed above in connection to Figure 5(b). Transition rates from Jonauskas et al. (2004), Nahar (2006), and CHIANTI (Dere et al. 1997; Del Zanna et al. 2015) mostly agree with the present MCDHF values to within 20%, but for some of the results of Nahar (2006) the deviation is beyond 50% (e.g., 198 − 2, 12 − 4), while some of the CHIANTI values differ from the present values by larger than an order of magnitude (e.g., 53 − 1, 52 − 1, 52 − 2).

3.4. Lifetimes

The radiative lifetimes from the present MCDHF and MBPT calculations, which include the contributions from all possible E1, E2, E3, M1, and M2 radiative decays from the corresponding levels, are presented in Table 1.

It shows that lifetimes for the first excited-level $2s^22p^5\ ^2P_{1/2}$ are determined by the M1 transition to the ground state $2s^22p^5\ ^2P_{3/2}$. The other level lifetimes are mostly dominated by E1 transitions, but the E2 transition rates from some $2s^22p^43p$ levels to $2s^22p^5$ levels are not negligible, since their contributions may exceed 20%, as seen in Figure 6(a). With increasing Z, the E2 transition rates from a few $2s2p^53d$ levels to $2s^22p^5$ levels can also exceed 10%, as shown in Figure 6(b).

The present MBPT and MCDHF lifetimes mostly agree to within 5%; the larger differences are due to the transition rates that have been discussed above. The present MCDHF lifetimes in L and V forms agree to within 2% for all the levels provided in Table 1.

4. SUMMARY

We have presented systematic MCDHF and MBPT calculations of energies and lifetimes for the lowest 200 levels arising from the $1s^22s^22p^5$, $1s^22s2p^6$, $1s^22s^22p^43l$, $1s^22s2p^53l$, $1s^22p^63l$, and $1s^22s^22p^44l$ configurations of F-like ions with $Z = 24$–30. Wavelengths, transition rates, oscillator strengths, and line strengths have also been provided for all transitions with a branching fraction larger than 1%.

The present two sets of energy levels show an average agreement to within 1000 cm^{-1} (0.02%), and most of the transition rates and lifetimes agree to within 5%. The present MCDHF results for the $n = 2$ complex are more accurate than the present MBPT results, while for higher n values, the present two sets of results have similar accuracy. Through our comparison, we can confidently point out some observations that may have large errors or incorrect identifications. We believe the present data could serve as benchmarks in future line identifications, and could make important contributions to diagnostics and modeling of astrophysical and fusion plasmas.

This work was supported by the National Natural Science Foundation of China under grant No. 11674066, No. 11504421, No. 11474034, and No. 11374062, China Scholarship Council (Grant No. 201608130201), Chinese Association of Atomic and Molecular Data, Training and Introducing Project of High-Level Innovative Talents of Hebei University for Promoting the Comprehensive Strength of the Midwest, and Swedish Research Council 2015-04842. It was also partially supported by the Chinese National Fusion Project for ITER under grant No. 2015GB117000 and the Shanghai Leading Academic Discipline Project under grant No. B107. R.S. would especially like to acknowledge the International Exchange Program Fund for Doctorate Students of Fudan University Graduate School. One of the authors (K.W.) expresses his gratitude for the support from the visiting researcher program at Fudan University.

Software: FAC (Gu 2005a, 2008; Gu et al. 2006), GRASP2K (Jönsson et al. 2013b), CHIANTI (Dere et al. 1997; Del Zanna et al. 2015) are used in the present work. We would like to thank the authors of these codes for providing support and guidance in using their codes.

REFERENCES

Badnell, N. R. 1986, JPhB, 19, 3827
Beiersdorfer, P., Träbert, E., Lepson, J. K., Brickhouse, N. S., & Golub, L. 2014, ApJ, 788, 25

Blackford, H., & Hibbert, A. 1994, ADNDT, 58, 101
Brage, T., & Fischer, C. F. 1993, PhyS, 1993, 18
Cheng, K., Kim, Y.-K., & Desclaux, J. 1979, ADNDT, 24, 111
Clementson, J., & Beiersdorfer, P. 2013, ApJ, 763, 54
Cornille, M., Dubau, J., Loulergue, M., Bely-Dubau, F., & Faucher, P. 1992, A&A, 259, 669
Curdt, W., Landi, E., & Feldman, U. 2004, A&A, 427, 1045
Del Zanna, G. 2006, A&A, 459, 307
Del Zanna, G., Dere, K. P., Young, P. R., Landi, E., & Mason, H. E. 2015, A&A, 582, A56
Dere, K. P., Landi, E., Mason, H. E., Monsignori Fossi, B. C., & Young, P. R. 1997, A&AS, 125, 149
Doschek, G. A., & Feldman, U. 2010, JPhB, 43, 232001
Dyall, K., Grant, I., Johnson, C., Parpia, F., & Plummer, E. 1989, CoPhC, 55, 425
Edlén, B. 1983, PhyS, 28, 51
Feldman, U., Curdt, W., Doschek, G. A., et al. 1998, ApJ, 503, 467
Feldman, U., Curdt, W., Landi, E., & Wilhelm, K. 2000, ApJ, 544, 508
Gordon, H., Hobby, M. G., & Peacock, N. J. 1980, JPhB, 13, 1985
Grant, I. P. 2007, Relativistic Quantum Theory of Atoms and Molecules: Theory and Computation (New York: Springer Science+Business Media, LLC)
Gu, M. 2005a, ADNDT, 89, 267
Gu, M. F. 2005b, ApJS, 156, 105
Gu, M. F. 2007, ApJS, 169, 154
Gu, M. F. 2008, CaJPh, 86, 675
Gu, M. F., Beiersdorfer, P., Brown, G. V., et al. 2007a, ApJ, 657, 1172
Gu, M. F., Chen, H., Brown, G. V., Beiersdorfer, P., & Kahn, S. M. 2007b, ApJ, 670, 1504
Gu, M. F., Holczer, T., Behar, E., & Kahn, S. M. 2006, ApJ, 641, 1227
Jonauskas, V., Keenan, F. P., Foord, M. E., et al. 2004, A&A, 416, 383
Jönsson, P., Alkauskas, A., & Gaigalas, G. 2013a, ADNDT, 99, 431
Jönsson, P., Gaigalas, G., Bieroń, J., Fischer, C. F., & Grant, I. 2013b, CoPhC, 184, 2197
Jönsson, P., He, X., Fischer, C. F., & Grant, I. 2007, CoPhC, 177, 597
Kallman, T. R., & Palmeri, P. 2007, RvMP, 79, 79
Kim, Y. K., & Huang, K. N. 1982, PhRvA, 26, 1984
Ko, Y.-K., Raymond, J. C., Li, J., et al. 2002, ApJ, 578, 979
Kramida, A., Ralchenko, Yu., Reader, J. & NIST ASD Team 2016, NIST Atomic Spectra Database (ver. 5.3) (Gaithersburg, MD: National Institute of Standards and Technology) available: http://physics.nist.gov/asd (2016 February 15)
Landi, E., & Phillips, K. J. H. 2005, ApJS, 160, 286
Lindgren, I. 1974, JPhB, 7, 2441
McKenzie, B., Grant, I., & Norrington, P. 1980, CoPhC, 21, 233
Mohan, M., & Hibbert, A. 1991, PhyS, 44, 158
Nahar, S. N. 2006, A&A, 457, 721
Nandy, D. K., & Sahoo, B. K. 2014, A&A, 563, A25
Ouart, N. D., Safronova, A. S., Faenov, A. Y., et al. 2011, JPhB, 44, 065602
Phillips, K. J. H., Fawcett, B. C., Kent, B. J., et al. 1982, ApJ, 256, 774
Safronova, A., Kantsyrev, V., Faenov, A., et al. 2012, HEDP, 8, 190
Safronova, M. S., Johnson, W. R., & Safronova, U. I. 1996, PhRvA, 53, 4036
Shestov, S., Reva, A., & Kuzin, S. 2014, ApJ, 780, 15
Si, R., Guo, X. L., Wang, K., et al. 2016, A&A, 592, A141
Sturesson, L., Jnsson, P., & Fischer, C. F. 2007, CoPhC, 177, 539
Sugar, J., & Musgrove, A. 1995, JPCRD, 24, 1803
Wang, K., Guo, X. L., Liu, H. T., et al. 2015, ApJS, 218, 16
Wang, K., Li, D. F., Liu, H. T., et al. 2014, ApJS, 215, 26
Wang, K., Si, R., Dang, W., et al. 2016, ApJS, 223, 3
Warren, G. A., Keenan, F. P., Greer, C. J., et al. 1997, SoPh, 171, 93
Witthoeft, M. C., Badnell, N. R., Del Zanna, G., Berrington, K. A., & Pelan, J. C. 2006, A&A, 446, 361
Witthoeft, M. C., Whiteford, A. D., & Badnell, N. R. 2007, JPhB, 40, 2969